Energy 49 (2013) 119–136

Contents lists available at SciVerse ScienceDirect

Energy

journal homepage: www.elsevier.com/locate/energy

A novel approach to multi-objective optimal power flow by a new hybrid optimization algorithm considering generator constraints and multi-fuel type

Mohammad Rasoul Narimani [a], Rasoul Azizipanah-Abarghooee [c,*], Behrouz Zoghdar-Moghadam-Shahrekohne [a], Kayvan Gholami [b]

[a] Department of Electrical and Electronics Engineering, Shiraz University of Technology, Shiraz, Iran
[b] Kermanshah Branch, Islamic Azad University, Kermanshah, Iran
[c] Department of Electrical Engineering, Marvdasht Branch, Islamic Azad University, Marvdasht, Islamic Republic of Iran

ARTICLE INFO

Article history:
Received 18 February 2012
Received in revised form
11 September 2012
Accepted 13 September 2012
Available online 14 November 2012

Keywords:
Optimal power flow
Multi-objective
Pareto optimal solution
Hybrid optimization algorithm
Particle swarm optimization
Shuffle frog leaping algorithm

ABSTRACT

This paper presents a new hybrid algorithm based on the Particle Swarm Optimization (PSO) and the Shuffle Frog Leaping algorithms (SFLA) for solving the Optimal Power Flow (OPF) in power systems. In consequence of economical issues and increasing of the social welfare, the OPF problem is turning into a pretty remarkable problem and getting more and more important in power systems. The proposed optimization problem has considered the real conditions of power generation involving the prohibit zones, valve point effect and multi-fuel type of generation units. Increasing concerns over the environmental issues forced the power system operators to consider the emission problem as a consequential matter beside the economic problems, so the OPF problem has become a multi-objective optimization problem. This paper takes advantages of the Pareto optimal solution and fuzzy decision making method in order to achieve the set of optimal solutions and best compromise solution, respectively. The presented algorithm is applied to 30, 57 and 118-bus test systems and the obtained results are compared with those in literature.

1. Introduction

The Optimal Power Flow (OPF) problem is one of the basic issues of power system operation and planning. The main target of the OPF problem is to find the optimal settings of the power system network in order to optimize a specific objective function while satisfying power flow equations and inequality constraints like system security and equipment operating limits [1,2]. During the years, a lot of methods have been applied to solve the OPF problem such as Non-Linear Programming (NLP) [3], Linear Programming (LP) [4,5], Newton methods [6,7] quadratic programming [8], integer programming [9], decomposition method [10,11] and fast successive linear programming algorithm [12]. The above methods can obtain the global optima in some cases, however these methods have some constraints like continuity and derivability of the objective function. Because of these reasons above methods are not suitable for solving the OPF problem. Therefore, it becomes essential to develop optimization techniques which are capable of overcoming these disadvantages and managing such difficulties. Over the last few years many population-based techniques are used to solve the complex constrained optimization problems and so their great efficiency is proved in solving these problems. For example, Niknam et al. presented a new model and a new developed population-based optimization method based on the charged system search algorithm to solve the highly nonlinear, non-continuous, non-smooth and non-convex dynamic OPF problem [13]. Duman et al. proposed a gravitational search algorithm to find the optimal solution for OPF problem in a power system [14].

Power plants generators usually have multiple valves in order to get the power output of the unit under control. When steam admission valves in thermal units are first opened, a sudden increase in losses is observed. This sudden increase leads to ripples in the cost function, which is known as the valve point loading effect. Also, in this paper prohibited zones constraint is considered beside the valve point effect. The prohibited zones arise from physical limitations of individual power plant components. Lee and Breipohl [15] give the example of the amplification of vibrations in a shaft bearing at certain operating regions. The aforementioned physical limitations may lead to instabilities in operation for certain loads. To avoid these instabilities, the concept of prohibited zones has been developed. The cost objective function is not continuous anymore when prohibited zones are taken into account. By considering the prohibited zones and multi-fuel type of units the cost objective function turns into a piecewise function. In point of fact all of the above constraints including valve

* Corresponding author. Tel.: +98 013 2546011; fax: +98 711 7353502.
E-mail address: razizipanah@gmail.com (R. Azizipanah-Abarghooee).

0360-5442/$ – see front matter © 2012 Elsevier Ltd. All rights reserved.
http://dx.doi.org/10.1016/j.energy.2012.09.031

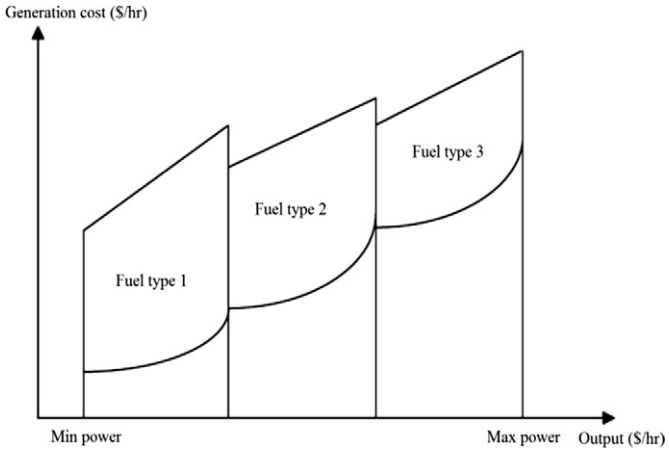

Fig. 1. Cost function curve related to the multi-fuel type.

point effect, prohibited zones and multi-fuel type cause the objective function to get more complicated, Meantime the number of the local optima is increased with considering above constraints. Therefore an accurate optimization algorithm is needed to solve the OPF problem. Over the past few years by introducing evolutionary optimization algorithms they are applied to complex optimization problems such as estimate energy demand problem [16], power system planning problem [17] and the OPF problem [2]. Among all of the evolutionary algorithms, Particle Swarm Optimization (PSO) algorithm is an accurate and reliable method which has been applied to variety of the optimization problems and its extraordinary ability in solving these problems has been demonstrated [18,19]. Like PSO algorithm, the Shuffle Frog Leaping Algorithm (SFLA) has proved its ability to find the proper solution in optimization problems [2,20]. Despite the privileges of the above algorithms, they have some drawbacks too like their trapping in local optima or converging to the global optima in long period of time. It is noteworthy to say that each evolutionary algorithm has a specific characteristic. For example, the PSO and the SFLA algorithms have a strong global search and local search, respectively. Therefore, for obtaining an accurate algorithm which has both search characteristics, the best way is to combine both the algorithms which are strongly proposed and precisely defined in this paper.

Over the last few years, rising concern over the environmental effect of fossil fuel and the passage of the US Clean Air Act amendments of 1990 forced the utilities to modify their operation strategies for generating the electrical power not only at minimum generation cost but also with minimum pollution level [21]. During the years some techniques have been presented to diminish the emission in power plant such as exchanging to low emission fuels [22], power producing with clean energy systems like photovoltaic, fuel cell and wind [23] and emission dispatching. The first two solutions require modification of the existing power plant or installation of some equipment which claims large investment. Therefore, the emission dispatch can be a more appropriate solution for reducing emission with respect to other methods. With considering the emission objective function beside the cost objective function, the OPF problem turns into a Multi-objective Optimization Problem (MOP) which is more complicated rather than a single objective OPF problem. Also, the MOP has a greater search space than the single objective problem, therefore necessity of an accurate optimization algorithm is more tangible respect before.

This paper presents a Hybrid Modified PSO-SFLA (HMPSO-SFLA) technique to cope with the complexity of the proposed algorithm. This algorithm profits the privileges of both PSO and SFLA algorithms. In addition, a new Self-Adaptive Probabilistic Mutation Operator (SAPMO) is implemented to increase the diversity of the generating population. The proposed SAPMO consists of four dominant strategies for moving each individual of the existing swarm. Each of these moving methods is recommended in order to handle one drawback associated with the original PSO algorithm. They enable the particles to use the best past experiences of the swarm and improve the diversity of the solutions. All of these mutation operators are necessary for complex optimization problems such as the OPF. To this end, a probability model based on the ability of each particle is implemented to provide a better corresponding solution in the entire search space of the problem. Since the presented problem is a MOP, it requires a multi-objective method for solving. During the years, some techniques have been recommended to solve the MOPs like reducing the MOP to a single objective problem by considering one objective as the target and others as the constraints [24]. Even if the emission is considered as objective, it can be translated to cost. In other word, the MOP of the OPF problem can be expressed as an economic single objective function (e.g. income) combining OPF (benefit) and OPF costs (disadvantage) and emission costs (disadvantage). The other methods augment all the objectives by dedicating a special weight to each objective function [25]. But these methods have some disadvantages like being dependent to the pre-determined weights which cause restriction on the available choices. Practically discussing, power generators would not aim at minimizing their emissions. Rather, their objective is to satisfy the emission constraints enforced by the government. This paper utilizes a Pareto-based approach which can obtain a set of optimal solutions instead one. The system operator can select one of these Pareto solution in which the emission constraints are satisfied. In this regard an external repository is defined to save all Pareto optimal solutions computed in each iterate of the optimization algorithm. Power system operators can select one of these solutions in accordance with their previous experience. Also this paper takes advantage of a fuzzy decision method to find the best Pareto optimal solution among all the Pareto solutions as the best compromise solution.

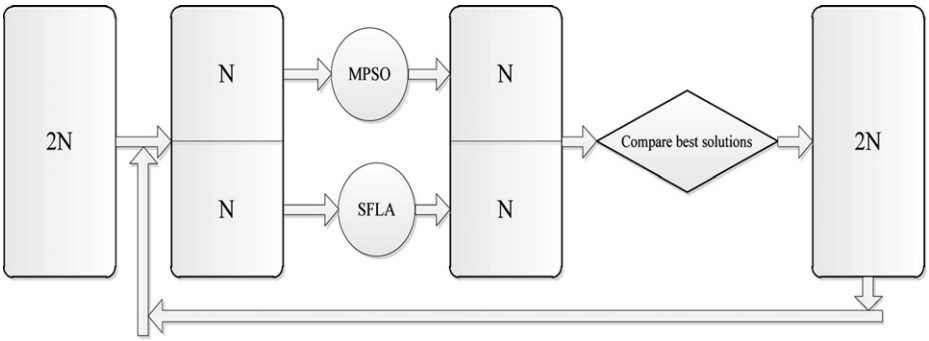

Fig. 2. Hybrid MPSO-SFLA diagram.

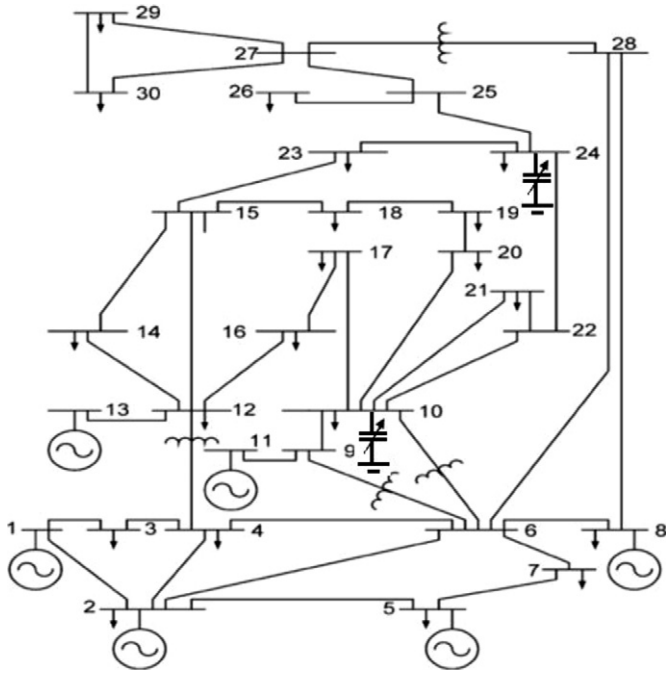

Fig. 3. One line diagram of 30-bus IEEE test system.

To verify the suitability of the presented algorithm it is applied to 30, 57 and 118-bus IEEE test systems. The obtained outcomes are compared with those in other literature. Simulation results prove the ability of the proposed algorithm in finding the global optima in the optimization problems since the presented algorithm can obtain better results with respect to the other algorithms.

The rest of this paper is organized as follow: Section 2 proposes the problem formulation and constraints, Section 3 presents the multi-objective solution strategy, Section 4 expresses the proposed hybrid optimization algorithm, Section 5 describes the implementation of the proposed algorithm on multi-objective OPF problem and Section 6 depicts simulation results.

2. Problem formulation

2.1. Generation cost objective function

The OPF problem is considered as a general minimization problem with constraints, and can be written in the following form [26,27]:

$$\min F_1(\mathbf{X}) = \sum_{i=1}^{N_g} a_i P_{gi}^2 + b_i P_{gi} + c_i + \left| d_i \times \sin\left(e_i \times \left(P_{gi}^{\min} - P_{gi}\right)\right)\right| \quad (\$/\mathrm{h}) \tag{1}$$

$$\mathbf{X} = [\mathbf{P_G V_G}, \mathbf{T}, \mathbf{Qc}] \tag{2}$$

where $F_1(\mathbf{X})$ is the total generation cost ($/h) [28], a_i, b_i, c_i, d_i, e_i are the cost function coefficients of the ith unit, P_{gi} is the real power generation of unit i, N_g is the total number of generation units. Also, $P_{gi}^{\min}$ is the minimum power generation limit for unit i. It should be noted that the control variables of the OPF problem are [$\mathbf{P_G}$, $\mathbf{V_G}$, $\mathbf{T}$, $\mathbf{Qc}$] where $\mathbf{P_G}$ is the vector of output generation of all generation units, $\mathbf{V_G}$ is the vector of voltage magnitudes for all the PV buses, $\mathbf{T}$ is the vector of tap transformers for all the transformers and $\mathbf{Qc}$ is the vector of reactive power output for all the compensator capacitors.

In Ref. [27] the reason of considering valve point effects in practical approaches has been explained. According to [27], it is worthwhile to note that the traditional cost function of each unit is presented in some literature as a quadratic function with smooth nature. But in reality, a sharp increase in fuel loss would be added to the fuel cost curve due to the wire drawing effects when steam admission valve starts to open. This procedure is named as valve point effects [27].

But definition of cost function in Equation (1) is related to the units with one type fuel, therefore this equation is not valid for multi-fuel type units. In real world, units might have some fuels as shown in Fig. 1. Thus, the cost function of multi-fuel type units can be defined as follow [26,29]:

$$F_1(\mathbf{X}) = \begin{cases} \sum_{i=1}^{N_g} a_{i,1}P_{gi}^2 + b_{i,1}P_{gi} + c_{i,1} + \left|d_{i,1} \times \sin\left(\left(e_{i,1} \times \left(P_{gi}^{\min} - P_{gi}\right)\right)\right)\right| & \text{if } P_{gi}^{\min} \le P_{gi} \le P_{gi,1}; \quad \text{fuel type 1} \\ \sum_{i=1}^{N_g} a_{i,2}P_{gi}^2 + b_{i,2}P_{gi} + c_{i,2} + \left|d_{i,2} \times \sin\left(e_{i,2} \times \left(P_{gi}^{\min} - P_{gi}\right)\right)\right| & \text{if } P_{gi,1} \le P_{gi} \le P_{gi,2}; \quad \text{fuel type 2} \\ \cdots\cdots\cdots\cdots\cdots & \\ \sum_{i=1}^{N_g} a_{i,Nf}P_{gi}^2 + b_{i,Nf}P_{gi} + c_{i,Nf} + \left|d_{i,Nf} \times \sin\left(e_{i,Nf} \times \left(P_{gi}^{\min} - P_{gi}\right)\right)\right| & \text{if } P_{gi,Nf-1} \le P_{gi} \le P_{gi}^{\max}; \quad \text{fuel type } Nf \end{cases} \tag{3}$$

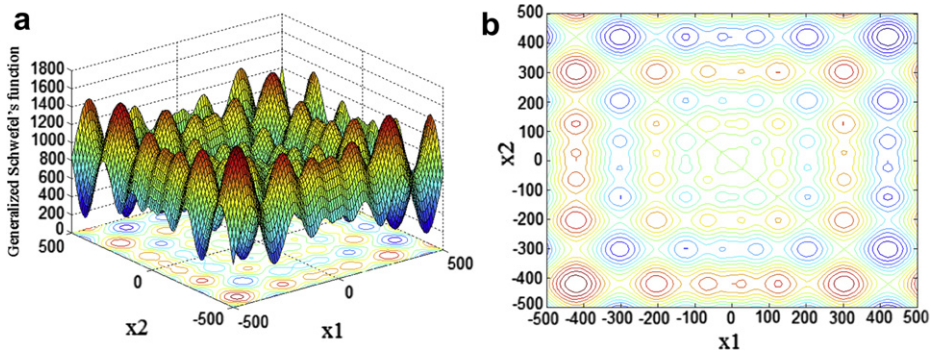

Fig. 4. a) 3D graph of Generalized Schwefel's function. b) Contour graph of Generalized Schwefel's function.

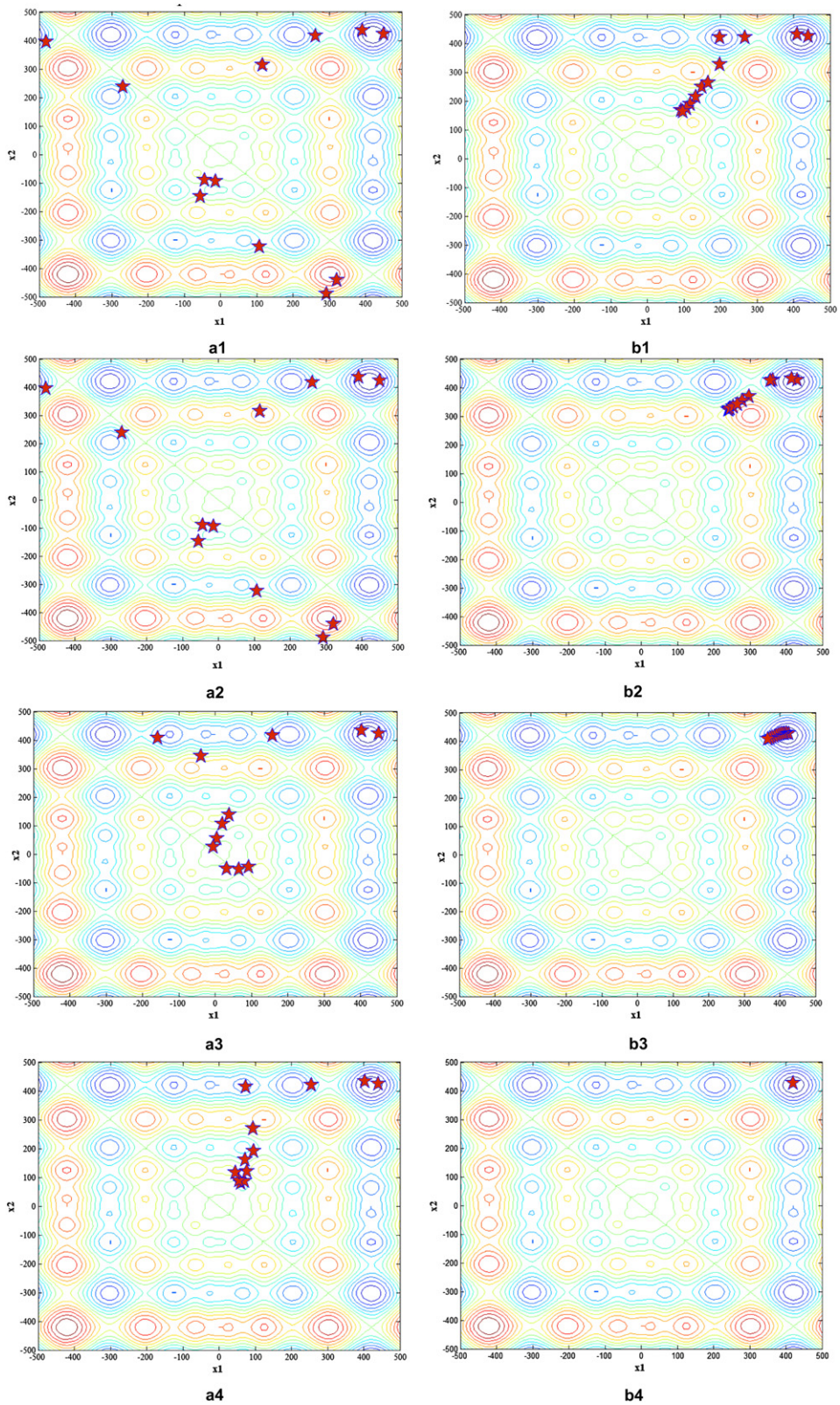

Fig. 5. a.1), a.2), a.3), a.4): Obtained results for the test function after the first iteration for respective SFLA, PSO, MPSO, and proposed PSO-SFLA. b.1), b.2), b.3), b.4): Obtained results for the test function after the final iteration for respective SFLA, PSO, MPSO, and proposed PSO-SFLA.

Table 1
Comparison of obtained results by different algorithms for cost objective function for test system 1 (Case I).

Algorithms	P_{g1} (MW)	P_{g2} (MW)	P_{g3} (MW)	P_{g4} (MW)	P_{g5} (MW)	P_{g6} (MW)	Total power (MW)	Loss (MW)	Cost ($/h)
EP [46]	173.85	50	21.39	22.63	12.93	12	292.79		802.62
TS [47]	176.04	48.76	21.56	22.05	12.44	12	292.85		802.29
IEP [48]	176.24	49.01	21.5	21.81	12.34	12.01	292.91	10.87	802.47
DE-OPF [49]	176.01	48.8	21.33	22.26	12.46	12	292.86	9.47	802.39
MDE-OPF [49]	175.97	48.88	21.51	22.24	12.25	12	292.85	9.46	802.38
GA [50]	192.51	48.4	19.55	11.62	10	12	294.07		804.11
SGA [50]	179.37	44.24	24.61	19.9	10.71	14.09	–		803.7
EGA [51]	176.2	48.75	21.44	21.95	12.42	12.02	–		802.06
ACO [52]	181.95	47	20.55	21.15	10.43	12.17	–	9.85	802.58
FGA [53]	175.14	50.35	21.45	21.18	12.67	12.11	–	9.49	802
GA-OPF [53]	174.83	48.88	23.78	20.2	13.14	12.22	–		803.92
MSFLA [2]	179.19	48.98	20.45	20.92	11.58	11.95	293.09	9.69	802.287
EP-OPF [49]	175.03	48.95	21.42	22.7	12.9	12.1	–		803.57
SFLA	181.06	52.17	22.47	15.35	10	12.07	293.12	9.72	802.21
PSO	180.23	52.09	22.81	15.62	10	12.21	292.96	9.56	801.89
Hybrid MPSO-SFLA	180.53	52.09	22.78	15.49	10	12.05	292.94	9.54	801.75

where, $a_{i,Nf}$, $b_{i,Nf}$, $c_{i,Nf}$, $d_{i,Nf}$, $e_{i,Nf}$ are the cost function coefficients of the ith unit for the fuel type Nf and $P_{gi}^{\max}$ is the capacity of generating unit i.

2.2. Emission objective function

The emission objective function can be presented as the sum of all types of emission, such as NO_X, SO_X, etc., with suitable pricing or weighting on each pollutant emitted. In the proposed study, two important types of emission gases are taken into account. The amount of NO_X and SO_X emission is given as a function of generator output, that is, the sum of a quadratic and exponential function as follows [28,30]:

$$F_2(\mathbf{X}) = \sum_{i=1}^{N_g}\left(\gamma_i P_{gi}^2 + \beta_i P_{gi} + \alpha_i + \xi_i \exp(\lambda_i P_{gi})\right) \quad (\text{ton/h}) \tag{4}$$

where $F_2(\mathbf{X})$ is the total emission (ton/h) [28], γ_i, β_i, α_i, ζ_i and λ_i are the emission coefficients of the ith unit.

2.3. Problem constraints

2.3.1. Prohibited operating zones

The cost curves of practical generators have prohibited operating zones due to some faults in the shaft bearing or vibration of machines or their accessories such as pumps or boilers [31,32]. A unit with prohibited operating zones has discontinuous input–output characteristics. It is necessary to determine a mathematic formulation for prohibited zones. Hence mathematically the feasible operating zones of unit can be depicted as follows:

$$P_{gi} \in \begin{cases} P_{gi}^{\min} \le P_{gi} \le P_{gi,1}^{L} \\ P_{gi,k-1}^{U} \le P_{gi} \le P_{gi,k}^{L}\, i = 1,\ldots,N_g; k = 2,\ldots,zi \\ P_{gi,k}^{U} \le P_{gi} \le P_{gi}^{\max} \end{cases} \tag{5}$$

Here zi is the number of prohibited zones in ith generator curve, k is the index of prohibited zone of ith generator, $P_{gi,k}^{L}$, $P_{gi,k}^{U}$ is the lower and upper bounds of the kth prohibited zone of unit i, respectively.

2.3.2. Equality and inequality constraints

The OPF equality constraints are related to the physics of the power systems. Also, the inequality constraints reflect the limits on physical devices in the power systems as well as the limits which are created to ensure system security. Equality and inequality constraints are defined as follow [33]:

$$P_i = P_{Gi} - P_{Di} = V_i \sum_{j=1}^{n} V_j (G_{ij}\cos\theta_{ij} + B_{ij}\sin\theta_{ij}) \quad i = 1,\ldots,n-1 \tag{6}$$

$$Q_i = Q_{Gi} - Q_{Di} = V_i \sum_{j=1}^{n} V_j (G_{ij}\sin\theta_{ij} - B_{ij}\cos\theta_{ij}) \quad i = 1,\ldots,n_{PQ} \tag{7}$$

$$P_{Gi,\min} \le P_{Gi} \le P_{Gi,\max} \quad i = 1,\ldots,N_g \tag{8}$$

Table 2
Control variables of different algorithms for cost objective function for test system 1 (Case I).

Algorithms	V_{g1}	V_{g2}	V_{g3}	V_{g4}	V_{g5}	V_{g6}	$TP_{6\text{-}9}$	TP_{6-10}	TP_{4-12}	$TP_{27,28}$	Q_{C10}	Q_{C24}	CPU time (sec)
EP [46]	1.05	1.036	1.005	1.016	1.069	1.055	1.02	0.9	0.95	0.94	–	–	–
TS [47]	–	–	–	–	–	–	–	–	–	–	–	–	–
IEP [47]	–	–	–	–	–	–	–	–	–	–	–	–	594.08
DE-OPF [49]	–	–	–	–	–	–	–	–	–	–	–	–	36.61
MDE-OPF [49]	1.05	1.038	1.011	1.019	1.095	1.084	0.987	0.971	0.997	0.941	–	–	23.07
GA [50]	–	–	–	–	–	–	–	–	–	–	–	–	–
SGA [50]	–	–	–	–	–	–	–	–	–	–	–	–	–
EGA [51]	1.05	1.038	1.012	1.02	1.082	1.067	1.013	0.95	1	0.963	–	–	–
ACO [52]	–	–	–	–	–	–	–	–	–	–	–	–	–
FGA [53]	1.05	1.034	1.006	1.003	1.071	1.048	1.003	0.965	1.016	0.965	–	–	–
GA-OPF [53]	–	–	–	–	–	–	–	–	–	–	–	–	–
MSFLA [2]	–	–	–	–	–	–	–	–	–	–	–	–	–
EP-OPF [49]	–	–	–	–	–	–	–	–	–	–	–	–	–
SFLA	1.05	1.043	1.026	1.031	1.05	1.05	1.1	1.2	0.9	0.97	11.35	13.84	20.75
PSO	1.05	1.047	1.019	1.024	1.05	1.05	1.2	1.1	1.1	0.96	12.08	14.42	20.19
MPSO-SFLA	1.05	1.048	1.022	1.027	1.05	1.05	1.2	1.1	1.2	0.97	12.17	14.83	18.17

Table 3
Comparison of obtained results by different algorithms for emission objective function for test sytem1 (Case I).

Algorithms	P_{g1} (MW)	P_{g2} (MW)	P_{g3} (MW)	P_{g4} (MW)	P_{g5} (MW)	P_{g6} (MW)	Emission (ton/hr)
MSFLA [2]	65.77	68.26	50	34.99	29.99	39.99	0.2056
SFLA [2]	64.48	71.38	49.85	35	30	39.97	0.2063
GA [2]	78.28	68.16	46.78	33.49	30	36.37	0.2117
PSO [2]	59.8	80	50	35	27.13	40	0.2096
Hybrid MPSO-SFLA	64.8148	68.0692	50	34.9999	30	40	0.2052

$$Q_{Gi,\min} \le Q_{Gi} \le Q_{Gi,\max} \quad i = 1,\ldots,N_g \tag{9}$$

$$|P_{ij}| \le P_{ij,\max} \tag{10}$$

$$V_{i,\min} \le V_i \le V_{i,\max} \quad i = 1,\ldots,n-1 \tag{11}$$

$$Q_{ci,\min} \le Q_{ci} \le Q_{ci,\max} \quad i = 1,\ldots,N_{\text{cap}} \tag{12}$$

$$T_{i,\min} \le T_i \le T_{i,\max} \quad i = 1,\ldots,N_{\text{tran}} \tag{13}$$

where, n is expressed as the number of the buses and $n-1$ is the number of the buses, excluding slack bus. n_{PQ} is the number of PQ or load buses. $\theta_{ij} = \theta_i - \theta_j$, that θ_i and θ_j are the voltage angle of two ending buses of an arbitrary branch. P_{Di} and Q_{Di} are the active and reactive power demand at bus i, respectively. $P_{Gi,\max}$ and $P_{Gi,\min}$ are the maximum and minimum active power generation values of ith bus, respectively. $Q_{Gi,\max}$ and $Q_{Gi,\min}$ are the maximum and minimum reactive power generation values of ith bus, correspondingly. P_{ij} is the power that flows between bus i and bus j. $P_{ij,\max}$ is the maximum power flows through the branch. V_i is the voltage magnitude of the ith bus, Q_{ci} is the reactive power of the ith compensator capacitor and T_i is the tap of the ith transformer. $V_{i,\max}$ and $V_{i,\min}$ voltages are respectively maximum and minimum valid voltages for each bus. $Q_{ci,\max}$ and $Q_{ci,\min}$ are the maximum and minimum reactive power output of the ith compensator capacitor, correspondingly. $T_{i,\max}$ and $T_{i,\min}$ are the maximum and minimum tap changing values of the ith tap transformer, respectively. N_{cap} and N_{tran} are the number of the compensator capacitor and the tap transformers, respectively.

3. Multi-objective solution strategy

MOP refers to the simultaneous optimization of multiple conflicting objectives, which produces a set of solutions instead of one particular solution while some constraints should be met. In fact, most of time, we find a set of solutions, owning to the contradictory objectives. MOP can be formulated as follows [34,35]:

$$\text{Minimize } F(\mathbf{X}) = \left(F_1(\mathbf{X}), F_2(\mathbf{X}), \ldots, F_{N_{\text{obj}}}(\mathbf{X})\right) \tag{14}$$

Subject to:

$$u_i(\mathbf{X}) < 0, \quad i = 1,2,\ldots,H \tag{15}$$

$$v_i(\mathbf{X}) < 0, \quad i = 1,2,\ldots,L \tag{16}$$

where, F_i is the ith objective function, $\mathbf{X}$ is a determination vector that presents a solution, N_{obj} is the number of objectives. L and H are the number of the equality and the inequality constraints, respectively.

3.1. Normalizing the objective function

The fuzzy decision making function as described in Equation (17) is implemented to normalize each objective function. μ_i is fully satisfied with related objective function if $\mu_i = 1$, and not satisfied at all if $\mu_i = 0$. Therefore, the value of each membership function shows the adaptability of the related objective [2,35].

$$\mu_i = \begin{cases} 1 & \text{if} \quad F_i \le F_i^{\min} \\ \dfrac{F_i^{\max} - F_i}{F_i^{\max} - F_i^{\min}} & \text{if} \quad F_i^{\min} < F_i < F_i^{\max} i = 1,\ldots,N_{\text{obj}} \\ 0 & \text{if} \quad F_i \ge F_i^{\max} \end{cases} \tag{17}$$

where, $F_i^{\max}$ and $F_i^{\min}$ are the acceptable maximum and minimum levels of objective function i, respectively.

3.2. Pareto optimal solution method

This paper utilizes the Pareto optimal solution method to achieve a set of solutions for the proposed problem. The Pareto method determines the squad of solution for multi-objective problems by applying the dominance concept. Each of the two proposed objective functionsF_1 andF_2 can have one of two possibilities: one of them dominates the other or none dominates the other. In other words, a vector dominates another one when it is less than or equal with respect to all of its components, and it is strictly less with respect to at least one of them. The definition of Pareto dominance for two decision vectors is described as follows [2,35]:

$$\begin{aligned} &\forall\ j \in \left\{1,\ldots,N_{\text{obj}}\right\}, F_j(\mathbf{X}_1) \le F_j(\mathbf{X}_2) \\ &\exists\ k \in \left\{1,\ldots,N_{\text{obj}}\right\}, F_k(\mathbf{X}_1) < F_k(\mathbf{X}_2) \end{aligned} \tag{18}$$

As mentioned before in this paper an external repository is defined for saving all non-dominated solutions during the optimization process. A candidate solution can be added to the repository if it satisfies any of the following conditions [35]:

- The repository is empty.
- The candidate solution dominates every single one of the solutions existing in the repository.

Table 4
Comparison of obtained results by different algorithms for cost objective function for test sytem1 (Case II).

Algorithms	P_{g1} (MW)	P_{g2} (MW)	P_{g3} (MW)	P_{g4} (MW)	P_{g5} (MW)	P_{g6} (MW)	Cost ($/h)
EP [46]	N/A	N/A	N/A	N/A	N/A	N/A	647.79
PSO	142.60	55	24.68	35	14.511	18.82	649.41
SFLA	140.68	65.87	25.45	35.00	10.00	16.12	654.47
Hybrid MPSO-SFLA	139.99	54.99	24.01	34.98	18.29	18.12	647.55

N/A: Not available in literature.

Table 5
Comparison of statistical results by different methods for cost objective function for IEEE 30-bus test system (sub-cases II.2).

Solution technique	Fuel cost ($)			CPU time (sec)
	Best value	Mean value	Worst value	
EP [46]	647.79	N/A	N/A	N/A
TS [47]	647.69	647.73	647.87	N/A
MDE-OPF [49]	647.846	648.356	650.664	37.05
DE [54]	650.8224	N/A	N/A	N/A
BBO [55]	647.7437	647.7645	647.7928	11.94
MPSO-SFLA	647.55	647.55	647.55	19.06

N/A: Not available in literature.

- The repository is not full and the candidate solution is not dominated by any of the solutions in the repository.
- The repository is full but the candidate solution is non-dominated and it is in a less crowded region than at least one of the existed solutions in the repository.

The solutions saved in this repository in all the iterations are sorted by a type of decision making method. In this regard the value of Equation (19) is computed for all the saved solutions in the repository and consequently the solution with the highest value is considered as the best compromise solution [35].

$$N_\mu(j) = \frac{\sum_{k=1}^{N_{obj}} \omega_k \times \mu_k(j)}{\sum_{j=1}^{m} \sum_{k=1}^{N_{obj}} \omega_k \times \mu_k(j)} \tag{19}$$

where, ω_k is the weight factor for the kth objective function and m is the number of the non-dominated solutions. In accordance with the importance of economic issues and environmental allowance, the weight factor (ω_k) can be selected by the operator. The solution with the maximum membership function N_μ is the most preferred compromise solution based on the adopted weight factors and selected as the best Pareto optimal solution or the final solution of the problem.

4. Proposed hybrid MPSO-SFLA algorithm

4.1. Modified particle swarm optimization

PSO is an evolutionary optimization method, which is inspired by social behavior of birds crowding or fish schooling [36]. A PSO algorithm consists of a population continuously updating the searching space knowledge. This population is formed by individuals, where each one represents a possible solution and can be modeled as a particle that moves through the hyperspace.

At each iteration k, each particle remembers its own best position associated with the best personal fitness value, $\mathbf{Pbest}_i^k$. The position with the best fitness value among all $\mathbf{Pbest}_i^k$ is denoted by $\mathbf{Gbest}^k$. Besides, the position and velocity of each particle are updated as follows:

$$\begin{aligned}\mathbf{V}_i^{k+1} &= \omega \mathbf{V}_i^k + C_1 rand(.)_1(\mathbf{Pbest}_i^k - \mathbf{X}_i^k) \\ &\quad + C_2 rand(.)_2\left(\mathbf{Gbest}^k - \mathbf{X}_i^k\right) i = 1, \ldots, N\end{aligned} \tag{20}$$

$$\mathbf{X}_i^{k+1} = \mathbf{X}_i^k + \mathbf{V}_i^{k+1}\ i = 1, \ldots, N \tag{21}$$

where, N is the number of the particles which constitute the population for the PSO algorithm. $\mathbf{V}_i^k$ and $\mathbf{V}_i^{k+1}$ are the velocity of the ith particle at kth and$(k+1)$th iteration, respectively. ω is an inertia weight, C_1, C_2 are the positive coefficients selected between 0 and 2 that $C_1+C_2 \le 4$. $rand(.)_1$ and $rand(.)_2$ are the random numbers in the range 0 and 1. Original PSO often suffers from the problem of being trapped in local optima so as to prematurely converge. A SAPMO is used in this paper to prevent this problem. In this regard mutant vectors $\mathbf{X}_{r1}$, $\mathbf{X}_{r2}$, $\mathbf{X}_{r3}$, $\mathbf{X}_{r4}$ are selected randomly from the existing population in order to uniformly cover the algorithm search domain. It is worthwhile to note that for increasing the mutation effect, each mutant vector is generated by different mutant rule as follow:

$$\begin{aligned}\mathbf{X}_{m,\text{mutant1}}^k &= \mathbf{X}_{r1}^k + rand(.)_1\left(\mathbf{Gbest}^k - \mathbf{X}_{r2}^k\right) \\ &\quad + rand(.)_2(\mathbf{X}_{r3}^k - \mathbf{X}_{r4}^k)\ m = 1, \ldots, N_{\text{mutant1}}\end{aligned} \tag{22}$$

$$\begin{aligned}\mathbf{X}_{m,\text{mutant2}}^k &= \mathbf{Gbest}^k + rand(.)_1(\mathbf{X}_{r1}^k - \mathbf{X}_{r2}^k) \\ &\quad m = 1, \ldots, N_{\text{mutant2}}\end{aligned} \tag{23}$$

$$\begin{aligned}\mathbf{X}_{m,\text{mutant3}}^k &= \mathbf{X}_m^k + rand(.)_1\left(\mathbf{Gbest}^k - \mathbf{M}^k\right) \\ &\quad m = 1, \ldots, N_{\text{mutant3}}\end{aligned} \tag{24}$$

$$\begin{aligned}\mathbf{X}_{m,\text{mutant4}}^k &= \mathbf{X}_{r1}^k + rand(.)_1(\mathbf{X}_{r2}^k - \mathbf{X}_{r3}^k) \\ &\quad + rand(.)_2(\mathbf{X}_{r1}^k - \mathbf{X}_{r4}^k)\ \ m = 1, \ldots, N_{\text{mutant4}}\end{aligned} \tag{25}$$

where, N_{mutant1}, N_{mutant2}, N_{mutant3} and N_{mutant4} are the numbers of particles which select the mutation strategy 1, 2, 3, and 4, respectively. $\mathbf{M}^k$ is the average value of the population in iteration k.

It should be noted that the mutation methods (22)–(24) can be considered as globally search correlated. They effectively improve the PSO's global optimization performance. The mutation method (25) is proposed to improve the diversity of the solutions, enhance the stagnation and avoid from the entrapping in the local optima.

The occurrence of mutation is followed by the requirements of the PSO search process. All the particles in the population will have a chance to be mutated, controlled by the probability of their methods of mutating. Based on a probability model, each particle selects one of these four methods. This probability model is based on the fitness of each particle to provide more optimal solutions. In the proposed MPSO algorithm, the first probability of all four mutation methods is 0.25 ($\text{Prob}_{\text{mutant},i} = 0.25$, $i = 1, 2, 3, 4$) and also a parameter is appropriated for each of these methods named accumulator in which the first value of this parameter is zero for all of these methods ($a_{\text{mutant},i} = 0$, $i = 1, 2, 3, 4$).

In each iteration, the population is sorted according to the fitness function shown in (26). The best particle is in the $n = 1$ place and the gloomy one is in $n = N$. Then, the weight factor (ww_n) is labeled for each of them. The better firefly corresponds to the

Table 6
Comparison of obtained results by different algorithms for cost objective function for test sytem1 (Case III).

Algorithms	P_{g1} (MW)	P_{g2} (MW)	P_{g3} (MW)	P_{g4} (MW)	P_{g5} (MW)	P_{g6} (MW)	Cost ($/hr)
SFLA	178.7488	45	21.751	24.7809	12.7991	12.619	812.8121
PSO	178.4547	45	21.9575	24.6522	12.9202	12.5332	812.2591
Hybrid MPSO-SFLA	178.19	49.36	21.82	25.05	12.78	12.25	811.2547

Table 7
Comparison of best compromise solution obtained by different algorithms for test system 1 (Case IV).

Algorithms	P_{g1}	P_{g2}	P_{g3}	P_{g4}	P_{g5}	P_{g6}	Cost	Emission
SFLA [2]	98.977	58.683	35.066	31.758	29.918	35.8174	872.853	0.2249
PSO	98.72	58.74	35.11	31.65	29.91	35.42	870.253	0.2248
Hybrid MPSO-SFLA	97.11	61.19	31.47	35	30	35.11	868.372	0.2246

higher value of ww_n. In the proposed approach, ww_n is calculated as follows:

$$ww_n = \frac{\log(N-n+1)}{\log(1)+\ldots+\log(N)} \quad n = 1,\ldots,N \tag{26}$$

The accumulator of each moving strategy is updated as follows:

$$a_{\text{mutant},i} = a_{\text{mutant},i} + \frac{ww_n}{N_{\text{mutant},i}} \quad 1,\ldots,N_{\text{mutant},i};\ i = 1,\ldots,4 \tag{27}$$

The excitation probability is formulated based on the above discussion as follows:

$$\text{Prob}_{\text{mutant},i} = (1-\rho)\text{Prob}_{\text{mutant},i} + \rho\frac{a_{\text{mutant},i}}{k_{\max}} \quad i = 1,\ldots,4 \tag{28}$$

where, $k_{\max}$ is the maximum number of iterations for the algorithm. ρ is a rate to control the speed of information exchanging in the MPSO algorithm. This parameter is dependent on the nature of the problem and tuned on the basis of some trial studies. The value of ρ is selected as 0.15, 0.167 and 0.142 in [27,37,38], respectively. ρ is set to 0.173 in this study. Finally, the roulette wheel mechanism is applied to choose the ith moving strategy for each particle based on normalized probability values. The values of normalized probability for each method of mutation are computed as follows:

$$\text{Prob}_{\text{mutant},i} = \frac{\text{Prob}_{\text{mutant},i}}{\sum_{i=1}^{4}\text{Prob}_{\text{mutant},i}} \quad i = 1,\ldots,4 \tag{29}$$

It should be considered that, after generating the mutant vectors we should check the limits for all the elements in each mutant vector to ensure that they do not break the limits, if any element of each vector breaks its limits ($x_{\max}$ or $x_{\min}$) it should be replaced by its related limit, which are the elements of upper and lower boundaries ($X_{\min}$, $X_{\max}$) of control vectors.

4.2. Shuffle Frog Leaping Algorithm (SFLA)

SFLA is a decrease based stochastic search method which begins with an initial population of frogs whose characteristics, known as memes, represent the decision variables. This algorithm contains elements of local search and global information exchange [20,39]. In SFLA, the total population is partitioned into groups (memeplexes) which these groups search independently. The procedure of partitioning is carried out by means of dividing of population into q memeplexes which each of the memeplexes contains p frogs. In this process, the first frog goes to the first memeplex, the second frog goes to the second memeplex, frog p goes to the qth memeplex, and $(p+1)$th frog goes back to the first memeplex, etc. In each memeplex, the frogs with the best and the worst fitness values are identified as $\mathbf{X}_b$ and $\mathbf{X}_w$, respectively. Also, the frog with the most qualified fitness level among all the memeplexes is identified as $\mathbf{X}_g$. Then, the following process is applied to improve only the frog with the worst fitness in each cycle. Accordingly, the position of the frog with the worst fitness is adjusted as follows:

$$\begin{aligned}\text{Change in frog position}(C_i) &= rand(.)_1(\mathbf{X}_b - \mathbf{X}_w)\\ &\quad + rand(.)_2(\mathbf{X}_g - \mathbf{X}_w)\end{aligned} \tag{30}$$

$$\begin{aligned}\text{New position } \mathbf{X}_w &= \text{current position of } \mathbf{X}_w + C_i;\\ &\quad -C_{\max} \le C_i \le C_{\max}\end{aligned} \tag{31}$$

where, $C_{\max}$ is the maximum allowed change in a frog position. If this process produces a better solution, it replaces the worst frog in each memeplex. If no improvement is achieved in this case, then a new population is randomly generated to replace that frog. The calculations then will continue for a specific number of iterations [40] and this procedure continues till the last iteration is accomplished.

4.3. Hybrid MPSO-SFLA

As mentioned before the PSO algorithm might be trapped in the local optima or converge to global optima in a long period of time. To cope with this problem this paper uses SFLA which has a strong

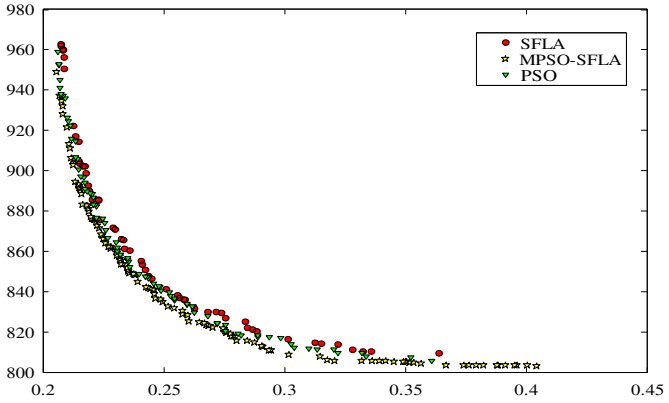

Fig. 6. Pareto front of IEEE 30-bus test system (sub-cases II.1).

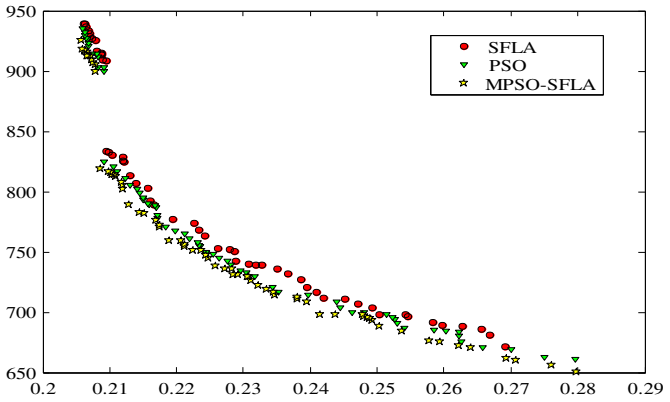

Fig. 7. Pareto front of IEEE 30-bus test system (sub-cases II.2).

local search ability. In this regard $2N$ population is generated at first and each algorithm starts its work with N population. After each iterate, the best solutions of both algorithms are compared and one with the minimum value is selected as the best solution for both algorithms in the next iteration. The schematic of algorithms hybridization is depicted in Fig. 2. The population should be sorted according to MAX-MIN method which is defined copiously in "Section 5. Step 6". Since the SFLA can amend the worst solutions in an effective way, worst solutions should be given to this algorithm and the best ones should be given to PSO algorithm.

5. Apply the hybrid MPSO-SFLA to proposed problem

To apply the hybrid MPSO-SFLA algorithm for solving the proposed problem, the following steps should be taken and repeated.

Step 1 The input data including the generators real powers, generators bus voltages, the fuel cost coefficients of the generators, the emission coefficients of the generators, the taps of the transformer, the reactive powers of switchable VARs, $F_i^{\min}$ and $F_i^{\max}$ are defined for $i = 1,2$.

Step 2 Transfer the constrained multi-objective problem to an unconstrained one as follow:

$$J(\mathbf{X}) = \begin{bmatrix} J_1(\mathbf{X}) \\ J_2(\mathbf{X}) \end{bmatrix}_{2\times 1} = \begin{bmatrix} F_1(\mathbf{X}) + L_1\left(\sum_{j=1}^{L}(v_j(\mathbf{X}))^2\right) + L_2\left(\sum_{i=1}^{H}(Max[0,-u_i(\mathbf{X})])^2\right) \\ F_2(\mathbf{X}) + L_1\left(\left(\sum_{j=1}^{L}(v_j(\mathbf{X}))^2\right) + L_2\left(\sum_{i=1}^{H}(Max[0,-u_i(\mathbf{X})])^2\right)\right) \end{bmatrix} \quad (32)$$

$v_j(\mathbf{X})$ and $u_i(\mathbf{X})$ are the equality and inequality constraints, respectively and L_1 and L_2 are the penalty factors.

Step 3 Produce the initial population

An initial population-based on the state variables is produced randomly as follow:

$$\text{Population} = \begin{bmatrix} \mathbf{X}_1 \\ \mathbf{X}_2 \\ \dots \\ \mathbf{X}_{2N} \end{bmatrix} \quad (33)$$

$$\mathbf{X}_i = \left[x_{i,1}, x_{i,2}, \dots, x_{i,N_{\text{param}}}\right] \quad (34)$$

$$\mathbf{X}_i = \left[\mathbf{P}_{\mathbf{G},i}\mathbf{V}_{\mathbf{G},i}, \mathbf{T}_i, \mathbf{Qc}_i\right] \quad (35)$$

$$x_{i,j} = rand(.)\left(x_{j,\max} - x_{j,\min}\right) + x_{j,\min}, j = 1, \dots, N_{\text{param}} \quad ; \quad i = 1, \dots, 2N \quad (36)$$

where, $x_{i,j}$ is the position of the jth control variable in the ith particle, $x_{j,\min}$ and $x_{j,\min}$ are the minimum and maximum limits of $x_{i,j}$, respectively. N_{param} and $2N$ are the number of control variables and the number of initial population, respectively.

Step 4 Calculate the objective functions values and normalize them by fuzzy decision making which is proposed in Equation (17). Also for each individual ($\mathbf{X}_i$) the membership values of all the different objectives are computed.

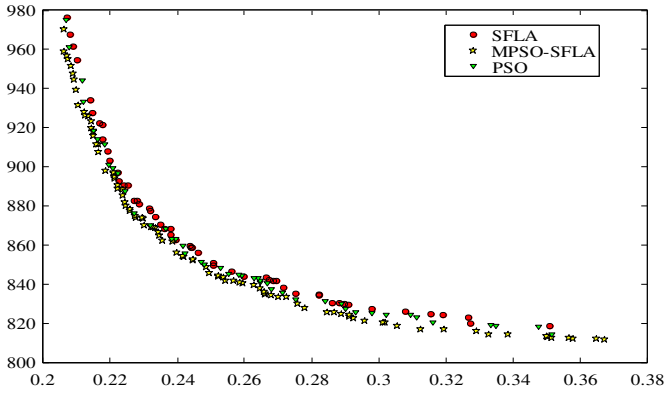

Fig. 8. Pareto front of IEEE 30-bus test system (sub-cases II.3).

Step 5 Apply the Pareto method and save non-dominated solutions in the repository.

Step 6 Update the parameters of the proposed algorithm.

Step 7 Select ($\mathbf{Pbest}_i^k$) and $\mathbf{Gbest}^k$ in each iterate as follow:

At first iteration initial population is considered as $\mathbf{Pbest}_i^k$ but in second to final iteration, if the $\mathbf{Pbest}_i^{k+1}$ dominate the $\mathbf{Pbest}_i^k$ then, the $\mathbf{Pbest}_i^k$ is replaced by $\mathbf{Pbest}_i^{k+1}$ and if it does not dominate $\mathbf{Pbest}_i^k$ then $\mathbf{Pbest}_i^k$ is remained as the best solution in next iteration for particle i. If none of them dominates each other, then $\mathbf{Pbest}_i^k$ is updated by MAX-MIN method in next iteration which is described as follow:

After computing all the objective functions and normalizing them by (17) in each iterate, then with calculating the following equation for all the objectives we can obtain μ_{Di} for each individual as follow:

$$\mu_{Di} = Min(\mu_1, \mu_2) \quad (37)$$

$$\mathbf{Pbest}_i^{k+1} = \begin{cases} \mathbf{X}_i^{k+1} & \text{if } \mu_{Di}(\mathbf{X}_i^{k+1}) > \mu_{Di}(\mathbf{Pbest}_i^k) \\ \mathbf{X}_{i,\text{mutant}}^k & \text{if } \mu_{Di}(\mathbf{X}_{i,\text{mutant}}^k) > \mu_{Di}(\mathbf{Pbest}_i^k) \\ \mathbf{Pbest}_i^k & \text{if } \mu_{Di}(\mathbf{Pbest}_i^k) > (\mu_{Di}(\mathbf{X}_i^{k+1}) \& \mu_{Di}(\mathbf{X}_{\text{mutant}}^k)) \end{cases} \quad (38)$$

But for selecting the $\mathbf{Gbest}^k$ in each iterate, the proposed procedure differs from the aforementioned procedure for $\mathbf{Pbest}_i^k$. Since the aim of this paper is finding the Pareto front for all the objective functions in order to cover and satisfy each objective in

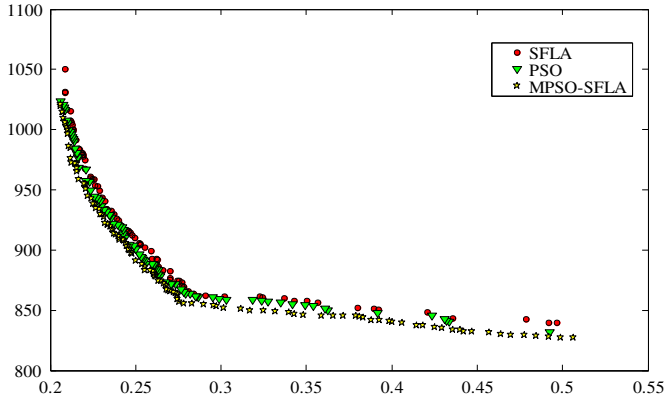

Fig. 9. Pareto front of IEEE 30-bus test system considering valve point effect.

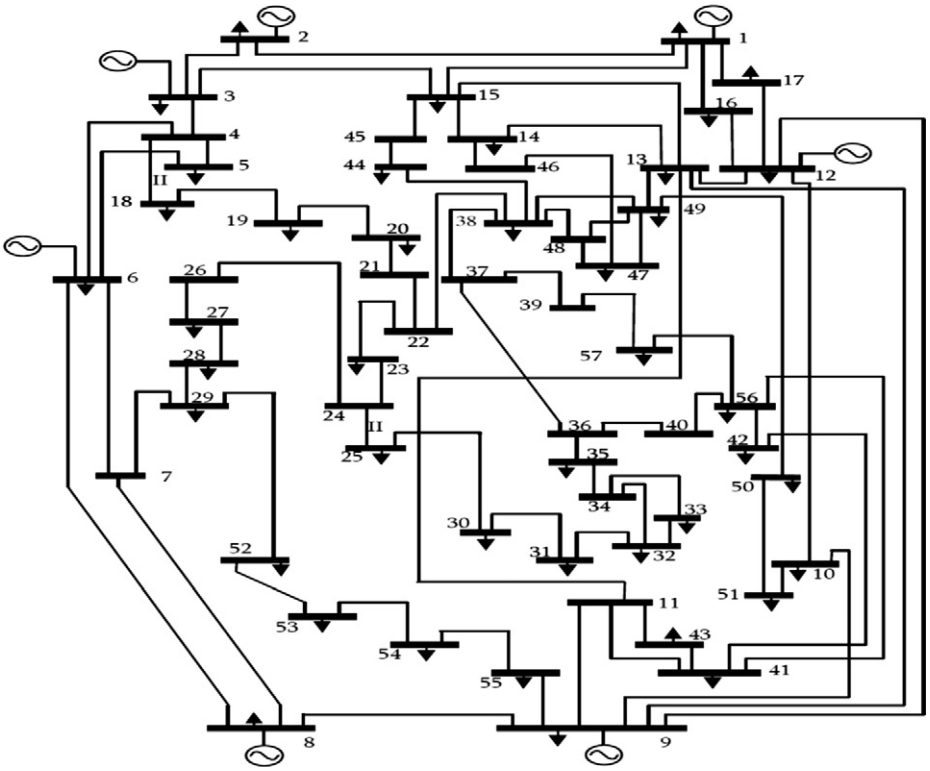

Fig. 10. One line diagram of 57-bus IEEE test system.

Pareto front, therefore a method should be implemented which considers all the objective values in obtaining Pareto front. In this regard the following procedure is fulfilled.

In the first k_{max}/Step iteration **Gbest**^{k} is defined as: all the individuals are sorted according to $F_1(\mathbf{X})$ value and the best individual is selected as **Gbest**^{k}, in the second k_{max}/Step individuals, **Gbest**^{k} is defined as: all the individuals are sorted according to $F_2(\mathbf{X})$ value and the best individual is selected as **Gbest**^{k}, in (N_{obj})th k_{max}/Step individuals, **Gbest**^{k} is defined as $F_{N_{obj}}(\mathbf{X})$ and in $(N_{obj}+1)$th k_{max}/Step individuals, **Gbest**^{k} is defined as $F_1(\mathbf{X})$ again, and so on.

Above procedure for comparing individuals is implemented to SFLA, it is worthwhile to note that there is no mutation in the SFLA algorithm. In other word max-min method is applied just for comparing SFLA individuals.

Step 8 Update the velocity and the position. The position and the velocity of each individual are modified by (20) and (21), respectively.

Step 9 If any element of each individual breaks its limits then the position of the individual is fixed to its maximum/minimum operating point.

Step 10 Compute the objective functions for the new generated individuals and normalize them.

Step 11 Apply the Pareto method and add the non-dominated solutions to the repository.

Step12 Determine the non-dominated solutions between the repository members by usage of the Pareto method. Because in each iterate some non-dominated solutions are added to the repository and they might dominate solutions which had been existed in the repository, therefore it is necessary to apply the Pareto method again to determine the real non-dominated solutions in the repository.

Step13 If the current iteration number obtains the pre-determined maximum iteration number, the algorithm, is stopped, otherwise go to step 6.

6. Simulation results

6.1. Test systems and parameters setting

In this section, the projected method is applied to four case studies to comprehensively investigate the performance of the proposed approach on the OPF problem. In this regard, these case studies are performed on 30, 57 and 118-bus IEEE test systems. The topology and the complete data of the IEEE 30, 57 and 118-bus test systems can be found in [41–43] and also all of them are described as follows:

6.1.1. Test system 1

The IEEE 30-bus test system consists of 6 generators, 41 lines, two capacitor banks and 4 transformers which are installed on the 6-9, 6-10, 4-12 and 27-28 branches. In the transformer tests, tap settings are considered within the interval [0.9, 1.1]. The available

Table 8
Comparison of obtained results by different algorithms for test system 2 considering cost objective function (Case IV).

	P_{g1}	P_{g2}	P_{g3}	P_{g4}	P_{g5}	P_{g6}	P_{g7}	Cost	Emission
Hybrid MPSO-SFLA	438.20	50.00	50.00	50.00	429.27	25.00	237.44	5137.56	4591.60
SFLA	438.47	50.00	50.00	50.00	430.01	25.00	237.12	5146.22	4593.82
PSO	438.51	50.00	50.00	50.00	429.42	25.00	237.79	5144.59	4594.37

Table 9
Comparison of obtained results by different algorithms for test system 2 considering emission objective function (Case IV).

	P_{g1}	P_{g2}	P_{g3}	P_{g4}	P_{g5}	P_{g6}	P_{g7}	Cost	Emission
SFLA	259.06	100.00	140.00	100.00	350.00	101.04	225.95	6543.28	3702.48
PSO	257.95	100.00	140.00	100.00	350.00	100.75	226.84	6539.95	3700.47
Hybrid MPSO-SFLA	258.54	100.00	140.00	100.00	350.00	100.00	226.34	6530.73	3697.56

reactive powers of capacitor banks are within the interval [0, 10] MVAr and they are connected to busses 10 and 24. Voltages are considered within the range of [0.95, 1.05]. The simulations search space has 17 dimensions for 30-bus IEEE test system, namely the 5 generators' active power, 6 generators' voltages, 4 transformers' taps, and 2 capacitors' banks. The one line diagram of IEEE 30-bus system is shown in Fig. 3 with a total load of 283.4 MW and 126.2 Mvar. The bus data and the branch data are taken from [41].

6.1.2. Test system 2

The simulations search space has 13 dimensions for 57-bus IEEE test system, namely the 6 generators' active power and 7 generator voltages. This test system include of 80 transmission lines, seven generators at the buses #1, #2, #3, #6, #8, #9 and #12, and 15 transformers. The shunt reactive power sources are considered at buses #18, #25 and #53. The total load demand of the system is 1250.8 MW and 336.4 MVAR. The data for this test system is provided from [42].

6.1.3. Test system 3

Finally, in order to demonstrate the scalability of the proposed approach, the scaling up performance is implemented and the OPF problem is solved for IEEE 118-bus test system. It is worthwhile to note that in this paper two types of 118-bus IEEE test system are considered which one of them has 54 generation units and other one has 19 generation units. The simulations search space has 107 and 37 dimensions for these test systems, respectively. The data for this test system is taken from [43].

It should be pointed out that the proposed work is implemented in MATLAB 7.6 computing environment with Pentium IV, 2.66 GHz computer with 512 MB RAM. MATPOWER [44] is a package of MATLAB m-files for solving power flow problem. It is intended as a simulation tool for researchers and educators which is easy to use and modify. In this paper we have changed the MATPOWER by adding MPSO-SFLA codes to solve proposed optimal power flow. In the implementation of MPSO-SFLA in the proposed problem, several parameters should be tuned for the optimal search process. In this paper, these parameters have been extracted from many simulation runs and experiments. The settings of the proposed algorithm are as follows:

- Number of population is set to 200 for all test systems.
- k_{max} is 100 for all test systems for single objective optimization problem. In addition, k_{max} is 200 for all test systems for multi-objective optimization problem.

Besides to get the optimal solution from the MPSO-SFLA, the setup for the proposed algorithm is described as following. The inertia weight factor is linearly decreased from 0.9 to 0.4, and C_1 and C_2 are both set to two for MPSO algorithm. In addition, the parameters required for SFLA algorithm are the number of frogs in each memeplex (p), number of memeplexes (q), number of iteration for local exploration which are set to 10, 10 and 70, respectively. It should be noted that due to the stochastic nature of the evolutionary algorithm, 30 independent trial runs are made to extract the statistical information.

6.2. Case studies

For comparison purposes, the single objective versions of the OPF have been solved. Then, the multi-objective OPF has also been solved. The rest of this section is organized as follow:

Case (I)
To demonstrate the convergence and robustness properties of the proposed MPSO-SFLA optimization algorithm, the well–known complex and non-smooth and multimodal Schwefel function has been used as test function.

Case (II)
This case includes 3 sub-cases for IEEE 30-bus test system, wherein the proposed MPSO-SFLA is compared with other evolutionary algorithms by solving different single objective OPF problems. The objective functions of this test case are cost function and emission (sub-case II.1), cost function with multi-fuel option (sub-case II.2) and cost function considering prohibited operating zones (sub-case II.3), respectively.

Case (III)
In this case, the multi-objective version of the OPF problem has been solved for all the IEEE 30, 57 and 118-bus test systems and the Pareto optimal front has been extracted.

6.2.1. Case (I): comparison of the proposed algorithm with different presented heuristic approaches via optimizing the Generalized Schwefel's function

The first test case of this section is an optimization problem with two decision variables x_1 and x_2 on Generalized Schwefel's function, presented in [45]. In Fig. 4, the objective function of the problem, which should be minimized, in terms of the decision variables x_1 and x_2 is shown. In this figure, different areas from the worst area to the best one are indicated by red, heavy yellow, light yellow and blue colors, respectively. As it can be seen, it is a nonlinear optimization problem with multiple local minima. The complexity of this test function is because of its deep local optima being far from the global optimum. It will be hard to find the global

Table 10
Comparison of best compromise solution obtained by different algorithms for test system 2 (Case IV).

	P_{g1}	P_{g2}	P_{g3}	P_{g4}	P_{g5}	P_{g6}	P_{g7}	Cost	Emission
Hybrid MPSO-SFLA	364.64	50.00	75.13	52.53	365.37	25.00	339.34	4775.68	4708.65
SFLA	364.20	50.00	75.33	52.90	365.52	25.00	339.49	4781.19	4709.11
PSO	364.57	50.00	75.28	52.63	365.73	25.00	340.05	4781.88	4718.83

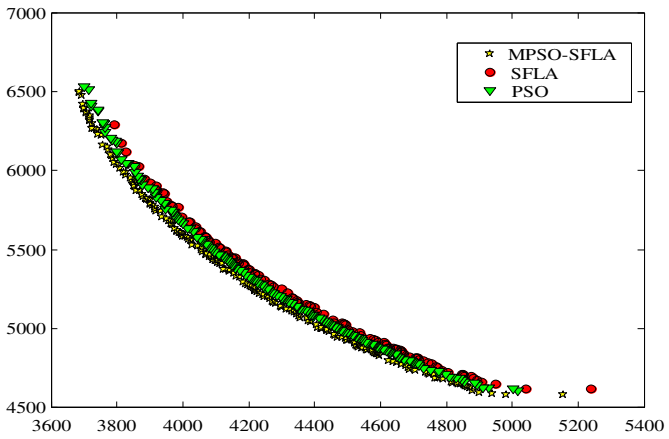

Fig. 11. Pareto front of IEEE 57-bus test system.

optimum if many particles fall into one of these local optima. Thus, the enhanced exploitation and exploration capabilities of the proposed MPSO-SFLA can appropriately be illustrated on it. The feasible region is restricted between −500 and 500 for all variables. As mentioned before, the 3D graph and the contour graph of the function are given in Fig. 4. The details of the test function used in this work are as following:

$$f(X) = \sum_{i=1}^{D}\left(-x_i \sin\left(\sqrt{|x_i|}\right)\right) + 418.983 \times D \tag{39}$$

where, D is the dimension of the test function and the optimum position of $X = [x_1, x_2]$ is [420.987, 420.987]. The optimum value for this test function at this point is zero.

To illustrate the enhanced exploitation and exploration capability of the proposed MPSO-SFLA with respect to each of the innovations which are applied to the original PSO and SFLA i.e. original SFLA, original PSO, MPSO, Fig. 5 is plotted. The iteration number and number of population are taken 30 and 12 for two dimensions, respectively. In this figure, the sample results of all the above methods for solving the Generalized Schwefel's function in two dimensional spaces of the decision variables are shown. The results of Fig. 5 have been obtained after the first and final iteration of each optimization method. It is clear that after the final iteration, all particles concentrate on the global optimum only for the proposed MPSO-SFLA. This figure clearly depicts that by applying each improvement to the original algorithms, the total performance is enhanced and better results are obtained step by step. By

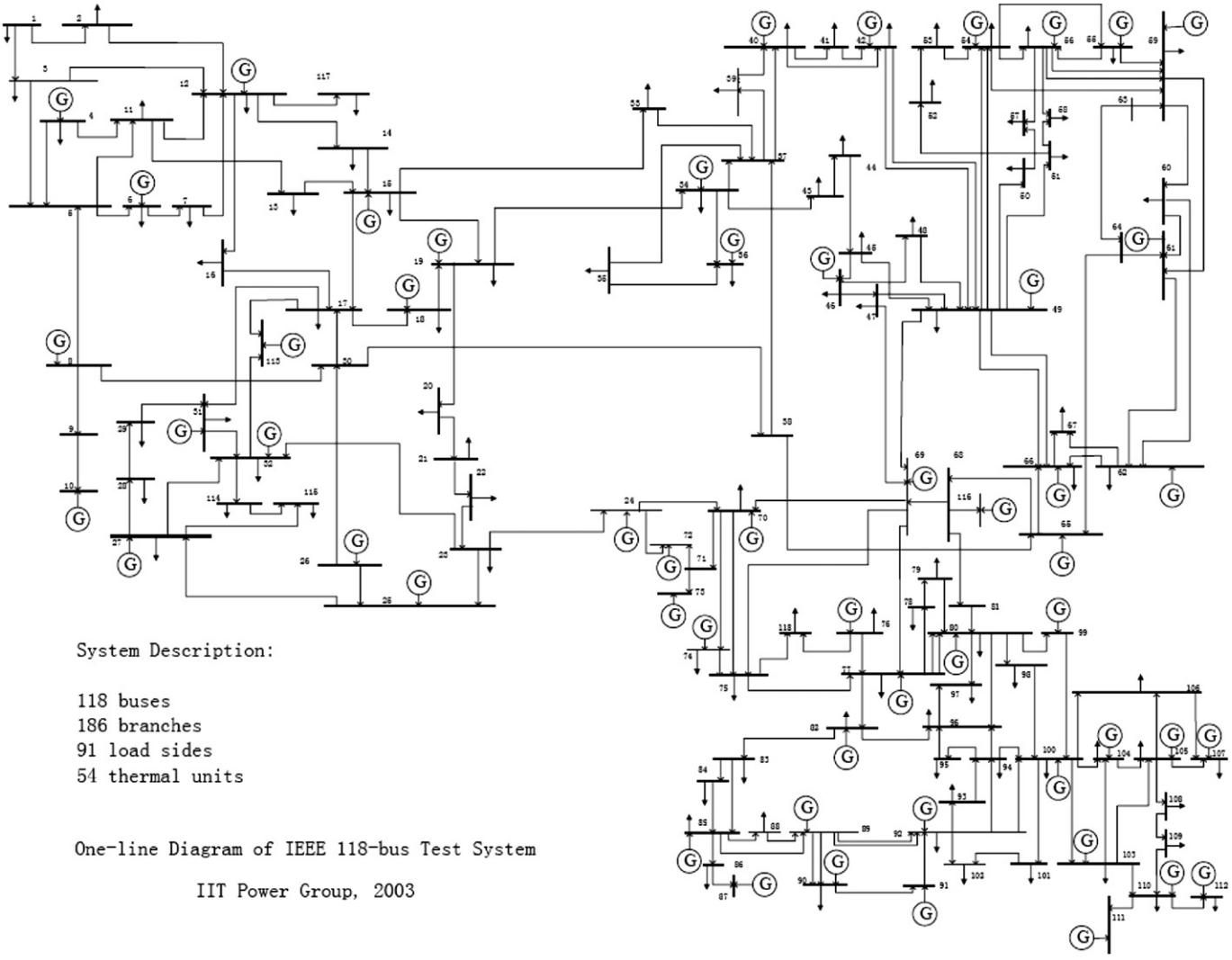

Fig. 12. One line diagram of 118-bus test system with 54 generators.

adding all improvements, good solutions for the MPSO-SFLA are achieved. This example illustrates high exploitation and exploration capability of the proposed algorithm for the local and global search of the promising area.

6.2.2. Case (II): comparison of the MPSO-SFLA with other solution methods (IEEE 30-bus test system)

6.2.2.1. Sub-case (II.1): original OPF without prohibited zones and multi-fuel. This case study is presented to prove the ability of the proposed algorithm in solving the optimization problem. As mentioned before in this case the original OPF problem is solved for test system 1, also the obtained results are compared with those in literature including Evolutionary Programming (EP) [46], Tabu Search (TS) [47], Improved Evolutionary Programming (IEP) [48], Differential Evolution Optimal Power Flow (DE-OPF) [49], Modified Differential Evolution Optimal Power Flow (MDE-OPF) [49], Genetic Algorithm (GA) [50], Stochastic Genetic Algorithm (SGA) [50], Enhanced Genetic Algorithm (EGA) [51], Ant Colony Optimization (ACO) [52], Fuzzy Genetic Algorithm (FGA) [53], Genetic Algorithm Optimal Power Flow (GA-OPF) [53] and Modified Shuffle Frog Leaping Algorithm (MSFLA) [2] which are shown in Tables 1 and 2. From these Tables it is clear that the proposed algorithm can obtain better results respect to other algorithms.

Also the emission objective function is optimized in this case and its obtained results are compared with the results of Shuffle Frog Leaping Algorithm (SFLA) and the Modified Shuffle Frog Leaping Algorithm (MSFLA) which are shown in Table 3. This table shows that the presented algorithm can obtain better results with respect to other algorithms.

6.2.2.2. Sub-case (II.2): OPF considering multi-fuel option. In this case study two generators including generator #1 and generator #2 of test system 1 have multi-fuel trends which can be found in [46]. It is clear that with considering multi-fuel type trends for these generators, the total generation cost is increased. The obtained results are depicted in Table 4 and also they are compared with those in literature including results of Evolutionary Programming (EP) [46], TS [47], MDE-OPF [49], DE [54] and Biography Based Optimization (BBO) [55]. The convergence characteristics of MPSO-SFLA and other methods i.e. EP [46], TS [47] MDE-OPF [49], DE [54] and BBO [55] are compared in Table 5 by calculating the statistical information of the solutions in 30 independent runs. It should be stressed that the worst value of the total cost obtained by the proposed method is better than the best solutions of all the other methods. Each algorithm that can achieve the lower objective function will be more effective. By comparing the best values of this table, the effectiveness of the proposed method is clearly specified. Also, the MPSO-SFLA obtains lower average cost than other methods, thus this will result in higher quality solution with respect to the other algorithms.

6.2.2.3. Sub-case (II.3): OPF considering prohibited operating zones. All generators in real world have prohibited zones in their generation limits, in order to illustrate this characteristic this paper proposed a discontinuous input–output characteristic which can be found in [39]. The obtained results are shown in Table 6 for generation cost objective function. It is clear that by considering prohibited zones the total generation cost is increased. Also it is noteworthy that the proposed algorithm coped with the discontinuous characteristics of the generators because all generators' outputs are in their limits.

6.2.3. Case (III): multi-objective optimal power flow

6.2.3.1. Sub-case (III.3): IEEE 30-bus test system. This case proposes multi-objective optimal power flow involving generation cost and emission objective functions. Since the single objective OPF problem is not acceptable anymore because of concerning about the environmental problems, so majority of OPF problems are inclined to the MOP which observes generation cost and emission objective functions simultaneously. As mentioned before this case solves the multi-objective OPF problem and also the obtained results are depicted in Table 7. Also, all Pareto plots are depicted in Fig. 6 for different algorithms. From this figure it is clear that Pareto solutions obtained by the proposed method dominate other Pareto solutions because this algorithm has a broad choice. In other word, the proposed technique can select more choices between limits of the choices and that is why its solutions have less emission and generation cost values. For evaluating the effects of different constraints on Pareto optimal solutions, Figs. 7–9 show the Pareto optimal fronts regarding these constraints. From these figures it is clear that the proposed algorithm can handle the MOP better than other algorithms which this proves the ability of the proposed algorithm once again.

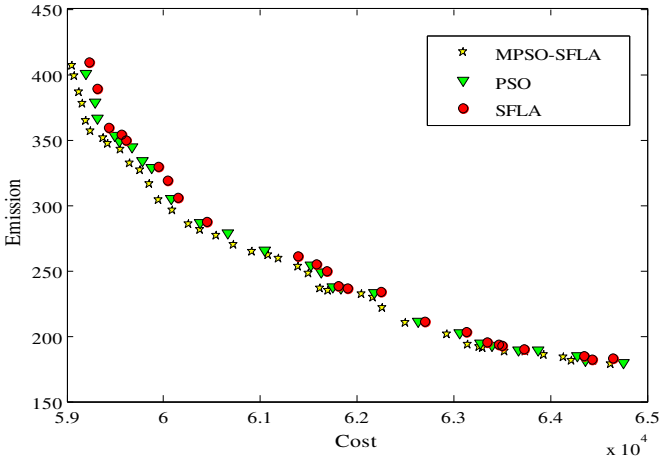

Fig. 13. Pareto front of IEEE 118-bus test system with 54 generators and linear model of emission.

6.2.3.2. Sub-case (II.3): IEEE 57-bus test system. In this section, 57-bus test system has been considered to illustrate the performance of the proposed algorithm. The one line diagram of the test system 2 is depicted in Fig. 10. The characteristics of this test system accompany with emission coefficients are given in [56]. The best solutions for cost and emission objective functions have been tabulated from Table 8–10. The obtained Pareto optimal solutions for different proposed optimization algorithms are shown in Fig. 11.

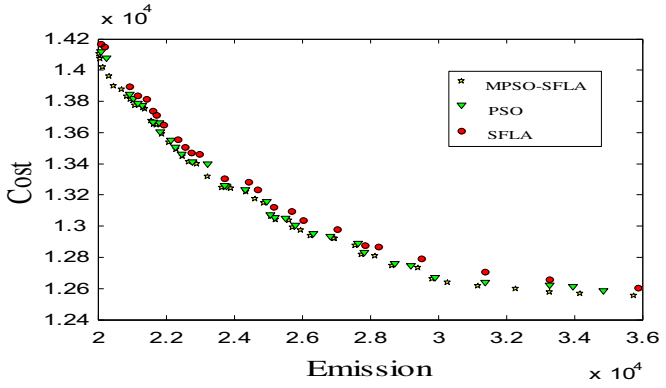

Fig. 14. Pareto front of IEEE 118-bus test system with 19 generators and non-linear model of emission.

Table 11
Emission coefficients for test system 3 with 54 generators.

Gen	Coefficient	Gen	Coefficient	Gen	Coefficient	Gen	Coefficient	Gen	Coefficient
G1	0.00	G12	0.00	G23	0.25	G34	0.15	G45	0.00
G2	0.00	G13	0.00	G24	0.25	G35	0.15	G46	0.00
G3	0.00	G14	0.00	G25	0.00	G36	0.00	G47	0.00
G4	0.00	G15	0.30	G26	0.00	G37	0.00	G48	0.00
G5	0.00	G16	0.30	G27	0.00	G38	0.00	G49	0.00
G6	0.00	G17	0.30	G28	0.20	G39	0.00	G50	0.00
G7	0.00	G18	0.30	G29	0.20	G40	0.00	G51	0.00
G8	0.35	G19	0.00	G30	0.20	G41	0.00	G52	0.00
G9	0.35	G20	0.00	G31	0.20	G42	0.00	G53	0.00
G10	0.35	G21	0.25	G32	0.15	G43	0.00	G54	0.00
G11	0.35	G22	0.25	G33	0.15	G44	0.00		

This figure expresses that the proposed optimization algorithm can obtain better solution respect the SFLA and the PSO algorithms, because the obtained results by the proposed algorithm can dominate the results obtained by the PSO and the SFLA algorithms. For one more time the efficiency of the algorithm is proved.

6.2.3.3. Sub-case (II.3): IEEE 118-bus test system. This case applies a proposed method for solving a multi-objective OPF in two different cases including IEEE 118-bus test system with 19 and 54 generators. The one line diagram for 118-bus test system with 54 generators is shown in Fig. 12. It is worthwhile to note that a linear emission model is implemented in this case. Two Pareto fronts related to two proposed test systems with 54 and 19 generators are shown in Figs. 13 and 14, respectively. The applied linear model of emission for 118-bus with 54 generators is defined as follows:

$$F_2(X) = \sum_{i=1}^{N_{gen}} \delta_i P_{Gi} \quad \text{lb/h} \tag{40}$$

where, δ_i is the emission coefficient related to the ith generator. Also, the emission coefficients can be found in [43] and also are shown in Table 11. Since the proposed model is simpler than (4) then the multi-objective OPF problem in which considers the emission according to Equation (40) will be less complex. Fig. 13 reveals the superiority of the proposed algorithm, because its obtained Pareto solution can dominate those obtained by other algorithms including SFLA and the PSO algorithms. Also the best solution of the proposed algorithm, SFLA and the PSO algorithms are shown in Tables 12, 13, 14 and 15 for 118-bus test system with 19 and 54 generators, respectively.

6.3. Comparative studies

6.3.1. Solution quality

Unlike in single objective optimization, performance evaluations to the MOPs are more complicated. This is because the optimization goal itself consists of the multiple objectives as follows: (i) Uniform diversity is desirable and (ii) Maximum extent of the obtained POF.

A study of the Figs. 6–9, 11, 13 and 14 shows that without using MPSO paralleled with the SFLA, PSO and SFLA methods, solutions get entrapped in the local optima and give the Pareto optimal front lower quality non-dominated solutions in comparison with the one

Table 12
Control variables of the best compromise solution obtained by different algorithms for test system 3-54 units (Case IV).

	Cost	Emission	Multi-objective		Cost	Emission	Multi-objective
P_{g1}	5.03	30.00	11.54	P_{g28}	318.68	100.00	208.53
P_{g2}	5.03	5.00	23.22	P_{g29}	111.23	80.00	80.00
P_{g3}	5.07	30.00	11.84	P_{g30}	30.06	30.00	75.39
P_{g4}	156.31	200.00	300.00	P_{g31}	10.02	10.00	30.00
P_{g5}	167.91	269.80	126.69	P_{g32}	5.00	5.00	16.32
P_{g6}	10.00	30.00	10.54	P_{g33}	5.01	5.00	5.00
P_{g7}	25.00	100.00	25.00	P_{g34}	25.06	25.00	33.27
P_{g8}	5.04	5.00	5.75	P_{g35}	25.13	25.00	93.11
P_{g9}	5.03	5.00	8.97	P_{g36}	150.22	237.78	220.00
P_{g10}	116.78	100.00	115.65	P_{g37}	25.11	100.00	41.63
P_{g11}	350.00	100.00	122.25	P_{g38}	10.03	10.00	15.81
P_{g12}	8.02	8.00	8.95	P_{g39}	186.61	100.00	108.50
P_{g13}	8.01	30.00	11.14	P_{g40}	95.09	200.00	100.00
P_{g14}	25.05	25.00	31.12	P_{g41}	9.11	12.02	14.16
P_{g15}	8.00	8.00	9.15	P_{g42}	20.01	20.00	31.22
P_{g16}	25.01	25.00	32.52	P_{g43}	109.67	200.00	153.48
P_{g17}	8.00	8.00	26.97	P_{g44}	101.04	100.00	109.22
P_{g18}	8.01	8.00	8.68	P_{g45}	114.50	200.00	100.00
P_{g19}	25.06	100.00	100.00	P_{g46}	8.00	8.00	8.22
P_{g20}	250.00	250.00	250.00	P_{g47}	25.06	100.00	25.00
P_{g21}	249.90	50.00	100.53	P_{g48}	25.04	25.00	25.00
P_{g22}	25.00	25.00	25.24	P_{g49}	8.03	20.00	15.67
P_{g23}	25.02	25.00	6.66	P_{g50}	25.01	50.00	43.40
P_{g24}	195.60	50.00	50.64	P_{g51}	25.11	27.54	25.00
P_{g25}	199.66	200.00	200.00	P_{g52}	25.03	30.54	30.91
P_{g26}	25.04	100.00	41.46	P_{g53}	25.02	26.87	25.00
P_{g27}	324.35	420.00	460.00	P_{g54}	25.03	50.00	43.43

Table 13
Comparison of the best compromise solution obtained by the proposed algorithm for test system 3-54 units (Case IV).

	Cost objective	Emission objective	Multi-objective
Cost value	55993.37	65711.87	61144.14
Emission value	408.51	178.70	258.32

including the MPSO-SFLA. In addition, by comparing the obtained results of these three methods in these figures, it can be found that the obtained solutions by the proposed MPSO-SFLA are mostly non-dominated by those obtained through the other methods. Besides, the better results for the cost and emission objective functions given in Tables 1–4, 6, 8, 9, 13 and 15 are quite evident, as it can be seen, the best solutions for different techniques are almost identical. It can be deduced that the developed techniques have satisfactory diversity characteristics for the MOPs as the best solutions for individual optimization are obtained along with other non-dominated solutions in a single run.

Since one of the significant targets of the proposed approach is solving the multi-objective problem, then it is so important to use some criterions to authenticate the obtained Pareto optimal solutions and compare them with those which are obtained by PSO and SFLA optimization algorithms. In this regard this paper utilizes Generational Distance (GD), Spacing (SP) and Diversity metric (*D*-metric) criterions which are described as follows:

6.3.1.1. Generational distance (GD). The GD criterion is proposed by Van Veldhuizen and Lamont [53] to estimate the value of being far from the elements in the set of non-dominated vectors. This criterion is explained as follows:

$$\mathrm{GD} = \frac{\sqrt{\sum_{i=1}^{m} d_i^2}}{m} \tag{41}$$

where d_i is the Euclidean distance (measured in objective space) between each of these non-dominated solution vectors and the nearest member of the Pareto optimal set. It is noticeable to note that a value of GD = 0 indicates that all the generated elements are in the Pareto optimal set and consequently whatever this criterion is closer to zero it shows that all the generated elements are the closer to zero this criterion is, the closer all the generated elements are to the Pareto optimal set. Therefore the less value of this criterion is more acceptable and the related Pareto optimal solutions have better condition respect to those which have grater GD values.

6.3.1.2. Spacing (SP). Another important factor of the obtained Pareto solutions is the distribution of these solutions in the Pareto fronts. In this regard a criterion in which measures the variance range of neighboring vectors in the non-dominated solutions is proposed in [57]. Since the "beginning" and the "end" of the current Pareto front are well known, a suitably delineated metric judges how well the solutions in such front are scattered. This criterion is defined as follows:

$$\mathrm{SP} \triangleq \sqrt{\frac{1}{m-1}\sum_{i=1}^{m}\left(\overline{d} - d_i\right)^2} \tag{42}$$

where, $d_i = \min_j\left(\left|f_1^i(\overline{X}) - f_1^j(\overline{X})\right| + |f_2^i(\overline{X}) - f_2^j(\overline{X})| + \ldots + |f_{N_{\mathrm{obj}}}^i(\overline{X}) - f_{N_{\mathrm{obj}}}^j(\overline{X})|\right), i,j = 1,\ldots,m$, $\overline{d}$ is the mean of all d_i. A value of zero for this metric indicates that all members of the Pareto front are posited equidistantly. Therefore the less value of this metric is more desirable and it shows that the distances between the Pareto optimal solutions in a Pareto front are divided equally.

6.3.1.3. Diversity metric. This metric does not require any Pareto optimal front and is based on the Hamming and Euclidean distance between solutions. If there is m number of points on a Pareto front and the space is N-dimensional then centroid C_i for ith dimension is computed as follows [58]:

$$C_i = \frac{\sum_{j=1}^{m} x_{ij}}{m}, \quad \text{For } i = 1, \ldots\ldots, N_{\mathrm{obj}} \tag{43}$$

where, x_{ij} indicates the ith dimension of the jth point. So the diversity measuring D-metric is calculated as follows:

$$D - \mathrm{metric} = \sum_{i=1}^{N_{\mathrm{obj}}}\sum_{j=1}^{m}\left(x_{ij} - C_i\right)^2 \tag{44}$$

The larger this metric is, the closer all the generated elements are to each other. In other word the distances between Pareto optimal solutions in a Pareto front are less. Therefore the higher the value of this parameter shows the higher diversity of the obtained Pareto optimal solutions.

Table 16 depicts the obtained best, worst and average of GD, SP and D-metric for proposed algorithm, PSO and SFLA. From this table, it is clear that the proposed algorithm can obtain better Pareto front respect other algorithms, because the values of SP and GD for the proposed algorithm is less than those obtained by the PSO and the SFLA algorithms. Also the value of D-metric related to the proposed algorithm is greater than those obtained by the other algorithms. This table reveals the superiority of the proposed algorithm in solving the MOP for once again.

Table 14
Control variables of the best compromise solution obtained by the proposed algorithm for test system 3-19 units (Case IV).

	Cost ($/hr)	Emission (ton/hr)	Multi-objective		Cost	Emission	Multi-objective
P_{g1}	528.45	440.25	461.80	P_{g11}	400.00	400.00	395.13
P_{g2}	10.00	90.00	37.14	P_{g12}	400.00	386.64	372.32
P_{g3}	147.88	300.00	217.48	P_{g13}	900.00	581.16	864.69
P_{g4}	343.36	400.00	351.55	P_{g14}	600.00	231.47	361.53
P_{g5}	1.00	10.00	3.79	P_{g15}	1.00	5.00	5.00
P_{g6}	3.00	23.00	3.00	P_{g16}	700.00	419.28	695.01
P_{g7}	126.79	240.00	213.08	P_{g17}	188.32	300.00	184.54
P_{g8}	5.00	50.00	13.29	P_{g18}	5.00	50.00	5.43
P_{g9}	32.89	200.00	179.36	P_{g19}	4.00	40.00	10.62
P_{g10}	26.10	200.00	54.85				

Table 15
Comparison of the best compromise solution obtained by the proposed algorithm for test system 3-19 units (Case IV).

	Cost objective	Emission objective	Multi-objective
Cost value	12329.23	14245.13	12872.95
Emission value	36708.92	18701.13	28387.75

6.3.2. Computational efficiency

Fig. 15 shows the variation of the best solution of cost for IEEE 30-bus test system (sub-cases II.1) with the number of iterations in the population during search procedure for PSO, SFLA and MPSO-SFLA. The premature convergence of the PSO compared to the SFLA and SFLA with respect to MPSO-SFLA degrade their performances and reduce their search capabilities which lead to a higher probability of being trapped in local optima. Thus, the hybrid MPSO-SFLA method is faster and it has better convergence trend compared with other algorithms. Moreover, the value of the objective function settles at the minimum point after about 17 iterations, and does not vary thereafter while other algorithms converge to global point in about at least 23 iterations.

Table 17 depicts the CPU execution time of different algorithms for solving different cases. According this table, the proposed algorithm can converge to its global optima or near its global solution in a lower computation time. In other word, the proposed algorithm has a higher speed of convergence. Once again the superiority of the proposed algorithm in solving optimization problems is proved.

6.3.3. Robustness

The performance of meta-heuristic search based optimization algorithms is judged through many trials with different initial populations to measure the robustness of MPSO-SFLA. For discussion of the robustness of the proposed approach and comparison of it with other methods, the OPF is solved for IEEE 30-bus test system (sub-cases II.1) in 30 independent trial runs and the statistical information such as mean, best and worst solution has been extracted. The mean, best and the worst results of the proposed approach are 801.75, 801.75 and 801.75, respectively which are more superior to the results of MDE [49] approaches i.e. mean = \$802.382, best = \$802.376 and worst = \$802.404. As well as, the proposed approach obtains better results in lower CPU time with respect to MDE [49] (18.17s opposed to 23.25s). It is clear that MPSO-SFLA method produces the better results most consistently in less execution time. The same justification can be used for other test cases.

Moreover, in this study the error analysis is implemented to show the robustness of the proposed approach. The error is the average difference between the obtained best solution and the global solution which indicates the ability of each technique for reaching the global optima or near global optimum solution. To show the superiority of the proposed approach, the error index is implemented and calculated for each optimization method for IEEE 30-bus test system (sub-cases II.2). The corresponding error of the original SFLA, original PSO, EP [46], TS [47] MDE-OPF [49], DE [54], BBO [55] and MPSO-SFLA are \$6.92, \$1.86, \$0.24, \$0.14, \$0.296, \$3.2724, \$0.1937 and \$0.0000. The same justification can be applied to the other test cases.

According to the above discussions and comparisons, it can be concluded that MPSO-SFLA is better than other techniques for the high dimensionality and high constraints non-convex, non-smooth and nonlinear single objective and multi-objective OPF optimization problems because of better results and true Pareto optimal solutions. The Pareto optimal front is consisted of high quality, robustness and well distributed non-dominated solutions. Also, extreme points of the trade-off surface are extracted in one single run.

Table 16
The best, worst and average values of GD, SP and D-metric for different optimization algorithms in two dimensional Pareto fronts.

Algorithms		MPSO-SFLA			PSO			SFLA		
Objectives		Best	Average	Worst	Best	Average	Worst	Best	Average	Worst
Cost-emission	SP	0.252439	0.384520	0.637506	0.606702	0.813980	1.214970	1.617467	2.412578	3.128754
	GD	0.045948	0.091637	0.130741	0.131218	0.166521	0.203120	0.304781	0.351290	0.417720
	D-metric	171480.4	130768.1	86549.4	157865.8	125471.9	64880.234	119473.7	98116.2	51820.7

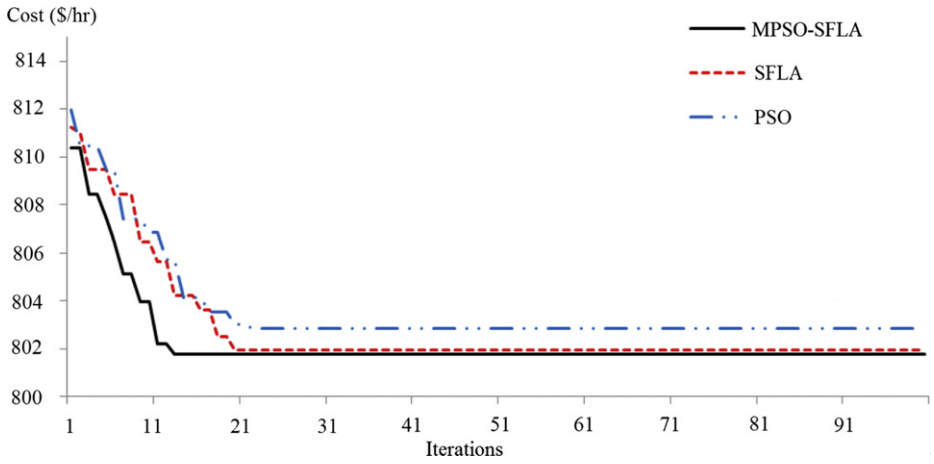

Fig. 15. Convergence graphs of MPSO-SFLA, original SFLA and original PSO for IEEE 30-bus test system (sub-cases II.1).

Table 17
Comparison of CPU time of different algorithms for different cases.

	PSO	SFLA	MPSO-SFLA
Sub-case (II.1)	21.84	19.22	18.17
Sub-case (II.2)	23.11	22.58	19.06
Sub-case (II.3)	24.94	24.74	20.65

7. Conclusion

The multi-objective optimal power flow has become one of the most popular optimization problems in power systems sector. By increasing concerns over the environmental issues these days, considering emission in power system operation problems has become more common respect before and that is why this paper proposed multi-objective OPF problem. Furthermore, in real world generators have some specific constraints such as prohibited zones which should be considered in optimization problem in order to have more real solutions, so these constraints are considered in this paper. Some generators work with multi-fuels which this means that generators have some cost functions instead one. Also this constraint is considered in this paper to cope with multi-fuels problem. In a word this paper presents the OPF problem which considers all constraints related to the generators and this indicates that this paper can observe as a comprehensive research in the OPF sector. The test results for the problem reveals the advantages of the proposed method in terms of speed of convergence, consistency, robustness and good Pareto optimal front. Consequently, the proposed approach can be a good candidate for real-time and real-size applications.

References

[1] Niknam T, Narimani MR, Aghaei J, Tabatabaei S, Nayeripour M. Modified honey bee mating optimisation to solve dynamic optimal power flow considering generator constraints. IET Gener Transm Distrib 2011;5:989–1002.
[2] Niknam T, Narimani MR, Jabbari M, Malekpour AR. A modified shuffle frog leaping algorithm for multi-objective optimal power flow. Energy 2011;36:6420–32.
[3] Momoh JA, El-Hawary ME, Adapa R. A review of selected optimal power literature to 1993. Part I: non-linear and quadratic programming approaches. IEEE Trans Power Syst 1999;14:96–104.
[4] Momoh JA, El-Hawary ME, Adapa R. A review of selected optimal power literature to 1993. Part II: Newton, linear programming and interior point methods. IEEE Trans Power Syst 1999;14:105–11.
[5] Lin QG, Huang GH, Bass B, Huang YF, Liu L. Optimization of energy systems under changing policies of greenhouse-gas emission control: a study for the province of Saskatchewan, Canada. Energy Sources 2010;32:1587–602.
[6] Ambriz-Perez H, Acha E, Fuerte-Esquivel CR, De La Torre A. Incorporation of a UPFC model in an optimal power flow using Newton's method. IEEE Proc Gener Transm Distrib 1998;145:336–44.
[7] Ambriz-Perez H, Acha E, Fuerte-Esquivel CR. Advanced SVC models for Newton-Raphson load flow and newton optimal power flow studies. IEEE Trans Power Syst 2000;15:129–36.
[8] Momoh JA, Guo SX, Ogbuobiri EC, Adapa R. The quadratic interior point method solving power system optimization problems. IEEE Trans Power Syst 1994;9:1327–36.
[9] Lin QG, Huang GH. A dynamic inexact energy systems planning model for supporting greenhouse-gas emission management and sustainable renewable energy. Renew Sust Energy Rev 2009;13:1836–53.
[10] Alsac O, Stott B. Optimal power flow with steady state security. IEEE Trans Power Appl Syst 1974:745–51.
[11] Ab Shoults R, Sun D. Optimal power flow based on P-Q decomposition. IEEE Trans Power Appl Syst 1982;101:397–405.
[12] Khaled Z, Sayah S. Optimal power flow with environmental constraints using a fast successive linear programming algorithm, applications to the Algerian power system. Energy Convers Manage 2008;49:3362–6.
[13] Niknam T, Azizipanah-Abarghooee R, Narimani MR. Reserve constrained dynamic optimal power flow subject to valve-point effects, prohibited zones and multi-fuel constraints. Energy 2012;47(1):451–64.
[14] Duman S, Güvenç U, Sönmez Y, Yörükeren N. Optimal power flow using gravitational search algorithm. Energy Convers Manage 2012;59:86–95.
[15] Lee FN, Breipohl AM. Reserve constrained economic dispatch with prohibited operating zones. IEEE Trans Power Syst 1993;8:246–54.
[16] Duran Toksar M. Ant colony optimization approach to estimate energy demand of Turkey. Energy Policy 2007;35:3984–90.
[17] Zhang D, Ma L, Liu P, Zhang L, Li Z. A multi-period superstructure optimisation model for the optimal planning of China's power sector considering carbon dioxide mitigation: discussion on China's carbon mitigation policy based on the model. Energy Policy 2012;41:173–83.
[18] Tichi SG, Ardehali MM, Nazari ME. Examination of energy price policies in Iran for optimal configuration of CHP and CCHP systems based on particle swarm optimization algorithm. Energy Policy 2010;38:6240–50.
[19] Unler A. Improvement of energy demand forecasts using swarm intelligence: the case of Turkey with projections to 2025. Energy Policy 2008;36:1937–44.
[20] Malekpour AR, Niknam T. A probabilistic multi-objective daily Volt/Var control at distribution networks including renewable energy sources. Energy 2011;36:3477–88.
[21] El-Keib AA, Ma H, Hart JL. Economic dispatch in view of the clean air act of 1990. IEEE Trans Power Syst 1994;9:972–8.
[22] Helsin JS, Hobbsm BF. A multi-objective production costing model for analyzing emission dispatching and fuel switching. IEEE Trans Power Syst 1989;4:836–42.
[23] Chel A, Tiwari GN, Chandra A. Simplified method of sizing and life cycle cost assessment of building integrated photovoltaic system. Energy Build 2009;41:1172–80.
[24] Granelli GP, Montagna M, Pasini GL, Marannino P. Emission constrained dynamic dispatch. Electr Power Syst Res 1992;1992(24):55–64.
[25] Coello CA, Christiansen AD. Multi objective optimization of trusses using genetic algorithms. Comput Struct 2000;75:647–60.
[26] Vaisakh K, Srinivas LR. A genetic evolving ant direction DE for OPF with non-smooth cost functions and statistical analysis. Energy 2010;35:3155–71.
[27] Niknam T, Azizipanah-Abarghooee R, Roosta A, Amiri B. A new multi-objective reserve constrained combined heat and power dynamic economic emission dispatch. Energy 2012;42:530–45.
[28] Niknam T, Narimani MR, Aghaei J, Azizipanah-Abarghooee R. Improved particle swarm optimisation for multi-objective optimal power flow considering the cost, loss, emission and voltage stability index. IET Gener Transm Distrib 2012;6:515–27.

[29] Amjady N, Nasiri-Rad H. Nonconvex economic dispatch with ac constraints by a new real coded genetic algorithm. IEEE Trans Power Syst 2009;24:1489–502.
[30] Vahidinasab V, Jadid S. Joint economic and emission dispatch in energy markets: a multiobjective mathematical programming approach. Energy 2010;35:1497–504.
[31] Niknam T, Doagou Mojarrad H, Zeinoddini Meymand H, Firouzi Bahman Bahmani. A new honey bee mating optimization algorithm for non-smooth economic dispatch. Energy 2011;36:896–908.
[32] Niknam T, Doagou Mojarrad H, Nayeripour M. A new fuzzy adaptive particle swarm optimization for non-smooth economic dispatch. Energy 2010;35: 1764–78.
[33] Salgado RS, Rangel Jr EL. Optimal power flow solutions through multi-objective programming. Energy 2012;42:35–45.
[34] Azizipanah-Abarghooee R, Niknam T, Roosta A, Malekpour AR, Zare M. Probabilistic multiobjective wind-thermal economic emission dispatch based on point estimated method. Energy 2012;37:322–35.
[35] Anvari Moghaddam A, Seifi A, Niknam T, Alizadeh Pahlavani MR. Multi-objective operation management of a renewable MG (micro-grid) with back-up micro-turbine/fuel cell/battery hybrid power source. Energy 2011;36: 6490–507.
[36] Nafar M, Gharehpetian GB, Niknam T. Improvement of estimation of surge arrester parameters by using modified particle swarm optimization. Energy 2011;36:4848–54.
[37] Niknam T, Azizipanah-Abarghooee R, Aghaei J. A new modified teaching-learning algorithm for reserve constrained dynamic economic dispatch. IEEE Trans Power Syst, in press.
[38] Niknam T, Azizipanah-Abarghooee R, Narimani MR. An efficient scenario-based stochastic programming framework for multi-objective optimal micro-grid operation. Appl Energy 2012;99:455–70.
[39] Niknam T, Narimani MR, Azizipanah-Abarghooee R. A new hybrid algorithm for optimal power flow considering prohibited zones and valve point effect. Energy Convers Manage 2012;58:197–206.
[40] Eusuff MM, Lansey KE. Optimization of water distribution network design using the shuffled frog leaping algorithm. J Water Res Pl Manage 2003;129:210–25.
[41] The University of Washington Electrical Engineering. Power system test case archive, the IEEE 30-bus test system data. Available at: http://www.ee.washington.edu/research/pstca/index.html; 2012.
[42] The University of Washington Electrical Engineering. Power system test case archive, the IEEE 57-bus test system data. Available at: http://www.ee.washington.edu/research/pstca/pf57/pg_tca57bus.htm; 2012.
[43] The Electrical and Computer Engineering Department, Illinois Institute of Technology, Data, The IEEE 118-bus test system data. Available at: http://motor.ece.iit.edu/data/JEAS_IEEE118.doc; 2012.
[44] The Power System Engineering Research Center. MATPOWER MATLAB toolbox. Available at: http://www.pserc.cornell.edu/matpower.html; 2012.
[45] Gong W, Cai Z, Ling CX, Li H. Enhanced differential evolution with adaptive strategies for numerical optimization. IEEE Trans Syst Man Cybern-Part B: Cybernetics 2011;41:397–413.
[46] Yuryevich J, Wong KP. Evolutionary programming based optimal power flow algorithm. IEEE Trans Power Syst 1999;14:1245–50.
[47] Abido MA. Optimal power flow using tabu search algorithm. Electr Power Components Syst 2002;30:469–83.
[48] Ongsakul W, Tantimaporn T. Optimal power flow by improved evolutionary programming. Electr Power Components Syst 2006;34:79–95.
[49] Sayah S, Khaled Z. Modified differential evolution algorithm for optimal power flow with non-smooth cost functions. Energy Convers Manage 2008;49:3036–42.
[50] Bouktir T, Slimani L, Mahdad B. Optimal power dispatch for large-scale power system using stochastic search algorithms. Int J Electr Power Energy Syst 2008;28:1–10.
[51] Bakistzis AG, Biskas PN, Zoumas CE, Petridis V. Optimal power flow by enhanced genetic algorithm. IEEE Trans Power Syst 2002;17:229–36.
[52] Slimani L, Bouktir T. Economic power dispatch of power system with pollution control using multiobjective ant colony optimization. Int J Comput Intell Res 2007;3:145–53.
[53] Saini A, Chaturvedi DK, Saxena AK. Optimal power flow solution: a GA-fuzzy system approach. Int J Emerg Electr Power Syst 2006;5:1–21.
[54] Abou El Ela AA, Abido MA, Spea SR. Optimal power flow using differential evolution algorithm. Electr Power Syst Res 2010;80:878–85.
[55] Bhattacharya A, Chattopadhyay PK. Application of biogeography-based optimization to solve different optimal power flow problems. IET Gener Transm Distrib 2011;5:70–80.
[56] Prabhakar Karthikeyan S, Palanisamy K, Rani C, Jacob Raglend I, Kothari D. Security constrained unit commitment problem with operational, power flow and environmental constraints. Wseas Trans Power Syst 2009;4:53–66.
[57] Coello Coello CA, Toscano Pulido G, Salazar Lechuga M. Handling multiple objectives with particle swarm optimization. IEEE Trans Evol Comput 2004;8: 256–79.
[58] Panigrahi BK, Ravikumar Pandi V, Das S, Das S. Multiobjective fuzzy dominance based bacterial foraging algorithm to solve economic emission dispatch problem. Energy 2010;35:4761–70.